Polymer Electrolyte Membrane (PEM) Fuel Cells: Automotive Applications

Shyam S. Kocha
Hydrogen Technologies and Systems Center,
National Renewable Energy Laboratory, Golden,
CO, USA

Article Outline

Glossary

Automotive PEMFC Proton exchange membrane fuel cell stacks used to power automotive vehicles typically using hydrogen as a fuel and ambient air as the oxidant

Electrocatalyst The material used on the anode and cathode electrodes of fuel cells to catalyze the fuel oxidation and oxygen reduction reactions to produce electrical power and by-products of heat and water. Amount of electrocatalyst used in the anode or cathode of fuel cells is reported in units of mg/cm^2

Fuel cell durability A measure of the degradation of components of a fuel cell as well as the output power of the entire stack over time. Also defined in terms of the maximum life of the stack before failure or degradation rate of the fuel cell performance in µV/h

Fuel cell performance The voltage produced by a fuel cell stack at a defined current density. A performance or polarization curve refers to a plot of the cell potential (V) versus current density (I) under specified conditions of pressure, temperature, humidity, and reactant stoichiometry

Membrane/PEM The proton conductive polymer electrolyte used to separate the anode and cathode compartments of fuel cells. The membrane replaces the liquid electrolytes used in some fuel cells.

Definition of Subject: Automotive PEM Fuel Cells

Since the discovery of fuel cells in the nineteenth century, they have been designed for operation with liquid alkaline, acid, and solid oxide ion conducting electrolytes in different temperature ranges to produce electrical power for stationary, portable, and automotive applications. The liquid acid that provides ionic conduction has been replaced by fairly thin proton conducting membranes such as polystyrenes and perfluorosulfonic acids (PFSAs) like Nafion and more recently with hydrocarbon-based polymers. These fuel cells incorporating a proton-conducting membrane rather than liquid electrolyte to separate the anode and cathode (forming a three-layer sandwich or catalyst coated membrane) are referred to as PEMFCs. PEMFCs are preferred for use in automotives for a multitude of reasons including their high volumetric and gravimetric power density.

PEMFCs for automotives have electrodes that are typically constituted of Pt-based catalysts separated by proton-conducting perfluorosulfonic acid (PFSA) or hydrocarbon membranes. The membranes (∼25 µm thick) have proton conductivities of about 100 mS/cm and areal resistances of 50 mΩ-cm^2. The anode Pt loadings that catalyze the hydrogen oxidation reaction (HOR) are of the order of 0.05 mg/cm^2, while the cathode Pt loadings that catalyze the oxygen reduction reaction (ORR) fall in the range 0.20–0.40 mg/cm^2. Automotive PEMFCs are

T. E. Lipman, A. Z. Weber (eds.), *Fuel Cells and Hydrogen Production*,
https://doi.org/10.1007/978-1-4939-7789-5_151

Originally published in
R. A. Meyers (ed.), *Encyclopedia of Sustainability Science and Technology*,

operated in the temperature range from ambient to ~90 °C at ambient to ~300 kPa and at 30–100% RH. Compressed hydrogen fuel tanks (350–700 kPa) and ambient air pressurized using a compressor are employed as the fuel and oxidant sources. Depending on the size of the vehicle, automotive fuel cell stacks produce 80–140 kW of peak power. Most fuel cell automotives are hybrids and employ a 10–20 kW NiMH or Li ion battery to improve efficiency and to store and provide supplemental power. Automotive PEMFCs are subject to variable operating conditions of high potentials, load cycling, start-up and shutdown cycles, humidity cycles, freeze-thaw cycles, and contamination from ambient air. The main obstacles toward commercialization of PEMFC stacks for automotives are the combination of cost, performance, and durability that are not mutually exclusive. Today's PEMFC-powered automobiles demonstrate driving ranges and lifetimes approaching (~70%) that of ICE vehicles. Major automotive companies have stated that PEMFCs for automotives are slated to arrive at cost levels approaching that necessary for commercialization beginning in 2015.

Currently, ICE-powered vehicles emit ~1.5 billion tons CO_2 equivalent per year at a US urban air pollution cost to society of $30 billion/year. The consumption of fossil fuels by the human species (~6.5 billion) has resulted in challenges of energy sustainability, environmental pollution, and global warming that need to be addressed urgently. Currently, several technologies that lower the greenhouse gas emissions partially such as gasoline-powered hybrid electric vehicles (HEVs) and gasoline plug-in hybrids (PHEVs), biofuel PHEVs, and batteries (BEVs) are being developed in parallel with fuel cells.

PEMFCs can operate on hydrogen fuel and atmospheric air to produce electrical energy, while exhausting only heat and water. Hydrogen is not available on earth as gas; it is found as a compound bound to oxygen as in water or bound to carbon, and in living things as biomass. Hydrogen is a carrier of energy and needs to be generated and stored efficiently; an infrastructure for hydrogen needs to be developed along with more efficient storage of hydrogen carried on board the vehicle. Currently about 9 million metric tons of hydrogen per year are generated in the USA that could power 30 million automobiles. Hydrogen can be produced from fossil fuels such as natural gas, and also, renewable sources, such as hydroelectric, wind, geothermal, solar photovoltaics, direct photoelectrochemical, and concentrated solar power ocean (tidal, wave, current, and thermal). The application of H_2|Air PEMFCs in automotives is one of the most important components in a renewable hydrogen economy that has the potential to reduce greenhouse gas emissions (to 80% below 1990 GHG levels), lower pollution, and arrest global warming.

Introduction

Fuel cells have been known to science for more than 150 years. In 1800, British scientists William Nicholson and Anthony Carlisle first demonstrated and explained the phenomena of using electricity to decompose water into hydrogen and oxygen. William Robert Grove (1811–1896), a Welsh scientist who was working on electrolysis of water to hydrogen and oxygen, tested the hypothesis that the reverse might be possible. He placed two platinum strips immersed in dilute sulfuric acid in two separate chambers, one of which was filled with hydrogen and the other with oxygen. A current was found to flow between the two platinum strips and water produced in the chamber confirming the hypothesis [1]. Although Grove was the first to build a working fuel cell, the discovery of the principle and fundamentals of the fuel cell is attributed to Christian Friedrich Schoenbein (1799–1868) [2]. Grove later improved on his original experiments by using a series of four cells to increase the total voltage; he named the device a "gas battery" – now known as a fuel cell stack.

Significant contributions were made in later years on fuel cells powered by various fuels such as that by Mond and Langer [3], Haber, W. V. Jacques [4], Bauer [5], Taitelbaum, Schmid [6], Tobler [7], and others. In addition to the experimental and practical fuel cell devices, a number of scientists contributed to the science and mechanism of the detailed functioning of fuel cells. Two noteworthy theories were debated to explain the functioning of the fuel cell. One was the “contact” theory originally proposed by Alessandro Volta (1745–1827) to explain his battery and the other was a “chemical” theory that held chemical reactions responsible for the generated power. Both theories had part of the solution which is that reactions that occurred where reactant gases, Pt catalyst, and electrolyte converged. This understanding was advanced by the contributions of Friedrich Wilhelm Ostwald (1853–1932). Other systematic nonempirical contributions were made by Nernst [8], Tafel [9], and Erdey-Gruz and Volmer. A history of the development of fuel cell electrodes between 1839 and 1960 can be found in the reviews of Liebhasvsky and Cairns [10], Vielstich [11], Baur [5], Tobler [7], Maget [12], and Liebhavsky and Grubb [13].

In 1932, Francis Thomas Bacon replaced the platinum electrodes with cheaper porous nickel metal and the sulfuric acid with potassium hydroxide to demonstrate the first alkaline fuel cell (AFC). Alkaline fuel cells were demonstrated to produce power for practical applications such as welding machines, tractors, powerlifts, etc., in the 1950s. Improved AFCs (2.3 kW) were engineered by Pratt & Whitney/International Fuel Cells (IFC) and were used by NASA in manned US Apollo space missions (1968–1972) and Skylabs for about 54 missions. High power density AFCs using precious metal-based catalysts, static electrolyte (KOH), and operating on hydrogen and oxygen have been used to power (three 12 kW stacks, 92 °C, 400 kPa) space shuttles since 1981 [14]. Other companies that have worked on AFCs include Union Carbide Corp., Siemens AG, and the European Space Agency [15].

Cation exchange resins polymerized as sulfonic acids became available in 1945 for use as deionizers. Around 1959, General Electric (Thomas Grubb and Leonard Niedrach) considered the use of these materials (sulfonated polystyrene) to form solid polymer electrodes (SPEs) as membranes for fuel cells; these materials were predicted to eliminate the system complexity involved in using liquid electrolytes and lead to the first PEMFCs [10, 16, 17]. The commercial availability of Teflon® (discovered in 1938 by Roy Plunkett of Dupont®) enhanced the performance of SPEs due to its hydrophobic nature and consequent lowered flooding of electrode pores. Using SPEs, PEM modules were fabricated and used in the Gemini space modules operating under hydrogen and oxygen. The Biosatellite 2 (1967) followed the Gemini program (seven flights, 1962–1966) in which Nafion membrane was used for the first time. GE continued working on PEMFCs and in the 1970s developed PEM water electrolysis technology for undersea life support that was used in US Navy oxygen-generating plants. Some of the technology from GE was acquired by UTC affiliates Hamilton-Standard and IFC in 1984. The British Royal Navy also adopted this technology in the 1980s for their submarine fleet. Siemens A.G. commenced a fuel cell research program on AFCs and in 1984 implemented a 100 kW fuel cell in a German navy submarine; they also have PEMFCs installed in submarines operating with rated power of 34–120 kW with technology that allows a high power density and good thermal management. The efforts described above in all these related areas established the basis and provided the foundation and grounds for pursuing fuel cells for automotive applications.

In 2009, ICE vehicles consumed about 3.5 billion barrels/year gasoline and emitted 1.5 billion tons CO_2 equivalent per year of the greenhouse gases [18]. Figure 1a illustrates the CO_2 emissions over the next century for five different scenarios and Fig. 1b illustrates the well-wheels greenhouse emissions projected for 2010 [19]. In the USA, 28% of the total energy used powers the transportation sector. The fuels commonly used for transportation are gasoline (62%), diesel (22%), jet fuel (9%), and natural gas (2%). The by-products (that have an impact on the environment and human health) of petroleum products include CO_2, CO, SO_2, NO_x, volatile organic compounds (VOCs), fine particulate matter (fine PM), lead, benzene, formaldehyde, acetaldehyde, 1,3 butadiene, etc. Automotives produce a large proportion of the pollution and greenhouse gases on earth;

with global warming becoming an accepted reality, governments and automakers are finally making an effort to lower greenhouse gas emissions. Although a number of intermediate low-emission technologies are being unraveled, PEMFCs are considered to be the best long-term solution since they can operate on hydrogen and atmospheric air to produce electrical energy, while exhausting heat and water with zero emissions.

Although onboard reforming of methanol, gasoline, etc., was seriously considered and attempted, fitting a miniature chemical plant in the limited space of a fuel cell vehicle was found to be untenable. Hydrogen was unanimously selected as the choice of onboard fuel for automotive vehicles in the early twenty-first century with an understanding of its strengths and weaknesses. Hydrogen is not available on earth as gas; it is found as a compound bound to oxygen as in water or bound to carbon, and in living things as biomass. Hydrogen has the highest energy content of any fuel by weight (hydrogen: 143 MJ/kg, gasoline: 43 MJ/kg) and the lowest by volume. Hydrogen can be produced from fossil, fuels such as natural gas, and renewable sources, such as hydroelectric, wind, geothermal, solar photovoltaics, direct photo-electrochemical, and concentrated solar power ocean (tidal, wave, current, and thermal). Hydrogen is also classified based on criteria such as primary energy sources (hydro, nuclear, wind, solar, natural gas, etc.); methods of production (reforming, electrolysis, etc.); and renewable/nonrenewable. Currently, about 9 million metric tons of hydrogen per year is generated ($\sim$95%-steam methane reforming (SMR) and the rest electrolysis); in the USA, this could, in principle, power $\sim$30 million automobiles.

Historically, there have been concerns about the safety of hydrogen, but in actuality, it is as safe and even safer than other flammable fuels such as gasoline and natural gas. A primary safety advantage of hydrogen is that it has very high diffusivity so that it dilutes rapidly to a nonflammable concentration in a reasonably ventilated space. Additionally, due to the absence of carbon and presence of water vapor in the combustion products of hydrogen, hydrogen fires release less radiant energy thus lowering incidents of secondary fires. The flammability limits, explosion limits, ignition energy, flame temperature, and stoichiometric mixture most easily ignited in air are all well documented for hydrogen. Codes and standards have been established for the safe use of hydrogen. Fuel cell vehicles are subjected to the same safety tests and crash/impact tests as gasoline-powered vehicles and have little trouble passing them.

As the world transitions to a hydrogen economy, a hydrogen infrastructure including a combination of distributed and centralized production is likely to evolve. Hydrogen pipeline networks already exist in some regions, often to provide hydrogen to the refining and food processing industry; transport by trucks is also prevalent. In the USA, at this time, there are 60 hydrogen fueling stations ($\sim$350 worldwide), 1,200 miles of hydrogen pipelines, and $\sim$9 million tons of hydrogen produced every year. Hydrogen storage is often categorized as physical (or molecular) and chemical (or dissociative) storage. Onboard physical storage methods include compressed gas, liquid hydrogen, and cryo-adsorbed hydrogen; chemical storage includes metal hydrides and liquid organic carriers. Typically, compressed hydrogen (35–70 MPa) in one or two tanks ($\sim$4–8 kg hydrogen depending on the target range) is stored onboard fuel cell vehicles today. Most fuel cell vehicles today closely meet the driving range of their IC engine counterparts.

The application of H_2|Air PEMFCs in automotives is one of the most important components in a renewable hydrogen economy that has the enormous potential to reduce greenhouse gas emissions (to 80% below 1990 GHG levels) and arrest global warming. Based on the Intergovernmental Panel for Climate Change (IPCC) study (Fig. 2) by 2050 well-wheels emissions of CO_2 must be reduced by 70% $\sim$ 90% versus 2000 levels [20]. Of all the possible pathways such as gas-electric hybrids, EVs, and fuel cells, only H_2|Air PEMFCs have the ability to reduce emissions to zero. Thus in attempts to reduce greenhouse gas emissions, lower dependence on imported oil, and limit urban air and water pollution, FCVs are expected to play a very central role.

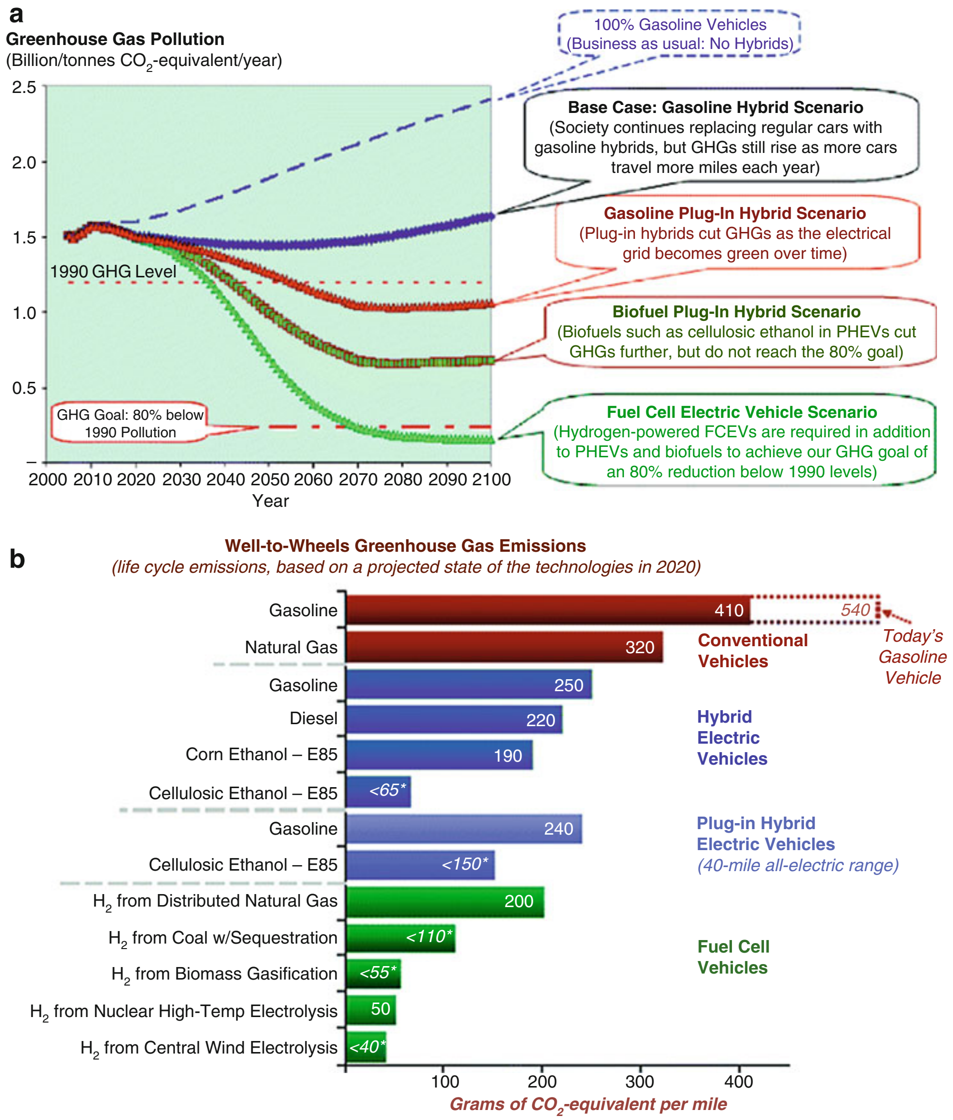

100% Gasoline Vehicles (Business as usual: No Hybrids)

Base Case: Gasoline Hybrid Scenario (Society continues replacing regular cars with gasoline hybrids, but GHGs still rise as more cars travel more miles each year)

Gasoline Plug-In Hybrid Scenario (Plug-in hybrids cut GHGs as the electrical grid becomes green over time)

Biofuel Plug-In Hybrid Scenario (Biofuels such as cellulosic ethanol in PHEVs cut GHGs further, but do not reach the 80% goal)

Fuel Cell Electric Vehicle Scenario (Hydrogen-powered FCEVs are required in addition to PHEVs and biofuels to achieve our GHG goal of an 80% reduction below 1990 levels)

Well-to-Wheels Greenhouse Gas Emissions
(life cycle emissions, based on a projected state of the technologies in 2020)

***Net emissions from these pathways will be lower if these figures are adjusted to include:**

- * The displacement of emissions from grid power–generation that will occur when surplus electricity is co-produced with cellulosic ethanol
- * The displacement of emissions from grid power–generation that may occur if electricity is co-produced with hydrogen in the biomass and coal pathways, and is surplus wind power is generated in the wind-to-hydrogen pathway
- * Carbon dioxide sequestration in the biomass-to-hydrogen process

Polymer Electrolyte Membrane (PEM) Fuel Cells: Automotive Applications, Fig. 1 (**a**) CO_2 emissions over the next century for five scenarios where gasoline vehicles, gasoline-hybrid, gasoline plug-in hybrids, biofuel plug-in hybrids, and fuel cell electric vehicles are used as the power source [18]; (**b**) well-wheels green house gas emissions based on state of technology in 2020 [19]

Brief History of Automotive Fuel Cells

Ballard should be recognized for reigniting the interest in PEMFCs in the late 1980s and 1990s and for the development of improved stacks used today by several companies in their fuel cell vehicles [21]. All the major automotive companies initiated fuel cell research and development programs as well as small-scale demonstration programs between 1998 and 2010; this was

Polymer Electrolyte Membrane (PEM) Fuel Cells: Automotive Applications, Fig. 2 Reduction in well-wheels CO_2 emissions recommended for 2050 by the Intergovernmental Panel for Climate Change (IPCC) study [20]

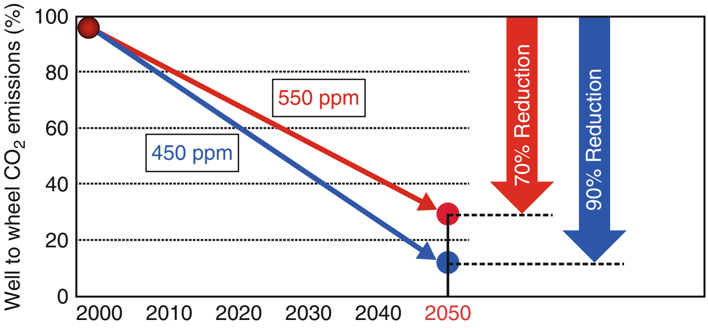

augmented by materials and component development by companies in the area of membranes, catalysts, diffusion media, bipolar plates, etc. In 2003, the US government announced a $1.2 billion FreedomCAR and Hydrogen Fuel Initiative (HFI) to develop hydrogen-powered fuel cells. Together, by 2008, the two initiatives invested about $1 billion to develop hydrogen-powered fuel cells, hydrogen infrastructure, and advanced automotive technologies. Fuel cells suffered a setback due to the 2009 US government policy that projected a longer 10–20-year forecast for automotive fuel cell commercialization. Nevertheless, most of the US, European, and Japanese automakers continue to support the development of PEMFCs for automotives internally as well as in public statements and most of the government funding was later restored. Also, in 2009, the European Union (EU) announced €140 million ($195 million) in available investments for research in energy technology. The funding (European Commission matched by contributions from the private sector) is part of a €1 billion ($1.4 billion) that the EU plans to invest in fuel cell research and development by 2014. In Japan, the Ministry of Economy, Trade and Industry (METI)'s New Energy and Industrial Technology Development Organization (NEDO) has overseen a lot of the funding for fuel cell and hydrogen research, development, and demonstration. The Japan Hydrogen & Fuel Cell Demonstration Project (JHFC) conducts research and activities for the practical use of fuel cell vehicles and hydrogen stations. The JHFC consists of the Fuel Cell Vehicle-Demonstration Study and the Hydrogen Infrastructures-Demonstration Study; the studies are subsidized by the METI. Many countries now have hydrogen corridors or hydrogen highways with a number of hydrogen fueling stations already implemented. In this section, for simplicity, the contributions made by a number of stack developers and automotive companies to advance fuel cell technology for automotives based on publicly available sources will be outlined.

Allis-Chalmers

In 1959, a team led by Harry Ihrig developed and demonstrated a 15 kW fuel cell tractor for Allis-Chalmers that was exhibited at state fairs across the USA. The FC stack system used KOH electrolyte and compressed hydrogen and oxygen as the reactants operating at 65 °C. The original fuel cell tractor is on display at the Smithsonian. In 1965, Allis-Chalmers further developed hydrogen-powered FC golf carts. Allis-Chalmers is also experimenting with fuel cell stacks to generate power for spot welders and forklift trucks.

General Motors

In 1968, GM's Electrovan was the automotive industry's first attempt at an automobile powered by a $H_2|O_2$ 125 kW fuel cell. It took a team of 250 people 2 years to demonstrate the potential feasibility of fuel cell technology. The Electrovan weighed more than twice as much as a normal van and could travel at speeds up to ~70 mph for 30 s. In the early 1980s, Los Alamos National Lab (LANL) initiated a PEMFC program and GM was part of the overview board. In 1996, the program moved from LANL to Rochester, NY, and later to Honeoye Fall, NY, where a large fuel cell R&D center still operates. In 1997, GAPC was formed globally at Honeoye Falls, NY; Mainz Kastel, Germany; Warren, MI; and

Torrance, CA. In 1998, the GM/DOE program was successful in demonstrating a 50 kW methanol fuel processor PEM system, and in late 1998, GM methanol Zafira was displayed at Geneva Auto Show. In 2000, focus shifted to hydrogen fuel, and in 2001, HydroGen 3, Zafira was launched. Figure 3 illustrates the history of the various GM FC vehicles from 1968 to 2001 and their latest FCV model. The advancements in volumetric and gravimetric power density of PEMFC stacks designed at General Motors between 1997 and 2004 are depicted in Fig. 4 [22]. Figure 5 is a photograph of their fifth generation stack [23]. GM's Chevrolet Equinox FCV passed 1 million miles with customers using the vehicles in everyday real-world conditions [24, 25]. GM and Honda have been working on fuel cells together since 2013 and the Honda-General Motors' partnership and cooperation on hydrogen fuel cells is approaching a new phase, as both parties intend to build a joint fuel cell plant for FCVs.

UTC Power/UTC Fuel Cells

For the last 40 years, various groups under the umbrella of United Technologies (IFC, UTC Fuel Cells, UTC Power) have been uninterruptedly involved in the research and development of fuel cell stacks such as the commercial PAFC stack-power plant and the AFC PEMFC stacks/power-plant used in the orbiter/space shuttle [26]. Over the last decade, UTC Power collaborated with several automotive companies to integrate their PEMFC stacks into various automotive platforms. Some of the interesting aspects of the UTC-PEMFC stack are that they operate close to ambient pressure and have unique water transport plates or separators; the plates are porous and have internal channels allowing for circulating water or coolant that performs the function of cooling the stack as well as passive water management. The reactants in the anode and cathode flow fields are, in principle, always humidified and improve the performance and durability of the membrane.

Some of the automotive companies they have worked with include: Hyundai-Kia Motor Company, Chevron Technology Ventures, Nissan, BMW, and a few others. UTC Power has also developed PEMFC 5 kW auxiliary power units APUs for BMW installed in BMW 7 series vehicles. The PEMFC stack APU provides energy for the vehicle's on-board electrical requirements. The third generation of the APU has been reported to perform for >3,000 h. UTC Power together with Hyundai-Kia Motor Company developed an automotive FCV that was capable of starting and functioning under subzero conditions; they were tested in the winter of 2008 in Michigan under the US DOE Hydrogen Fleet and Infrastructure Program. UTC Power also supplied PEMFC stacks for initial generations of Nissan X-TRAIL FCVs.

Ballard/AFCC

Ballard Power Systems was originally founded in 1979 as Ballard Research Inc. by Dr. Geoffrey Ballard to conduct research on high-energy lithium batteries. In the late 1980s and 1990s, Ballard championed PEMFCs for automotive and other uses and reinvigorated the field. In 1995, Ballard Systems tested PEM cells in buses in Vancouver and Chicago and later in experimental vehicles made by DaimlerChrysler. In late 2007, Ballard pulled out of the hydrogen vehicle sector of its business to focus on fuel cells for forklifts and stationary electrical generation. Established in 2008, the Automotive Fuel Cell Cooperation (AFCC) is a Burnaby, B.C.-based joint-venture private company owned by Daimler AG, Ford Motor Company, and Ballard Power Systems Inc. to develop fuel cell stacks for automotive applications. Today, Daimler and Ford have more than 150 fuel cell vehicles on the road. The fuel cell vehicles of Ford and Daimler are combined together in this subsection since they both generally utilize stacks based on AFCC technology.

DaimlerChrysler unveiled a series of FCVs using Ballard stacks such as the NECAR 1 (50 kW, Compressed H_2, 1994), NECAR 2 (50 kW, Compressed H_2, 1996), NECAR 3 (50 kW, liquid methanol, 1997), NECAR 4 (70 kW, liquid H_2, 1999), and F-Cell (A-class) FCV hybrid delivering 85 kW (Ballard Mark 900) using compressed H_2 in 2002. Most recently, Mercedes announced a series-production of B-class F-Cell powered by an electric motor that generates 136 hp. and 214 lb-ft of

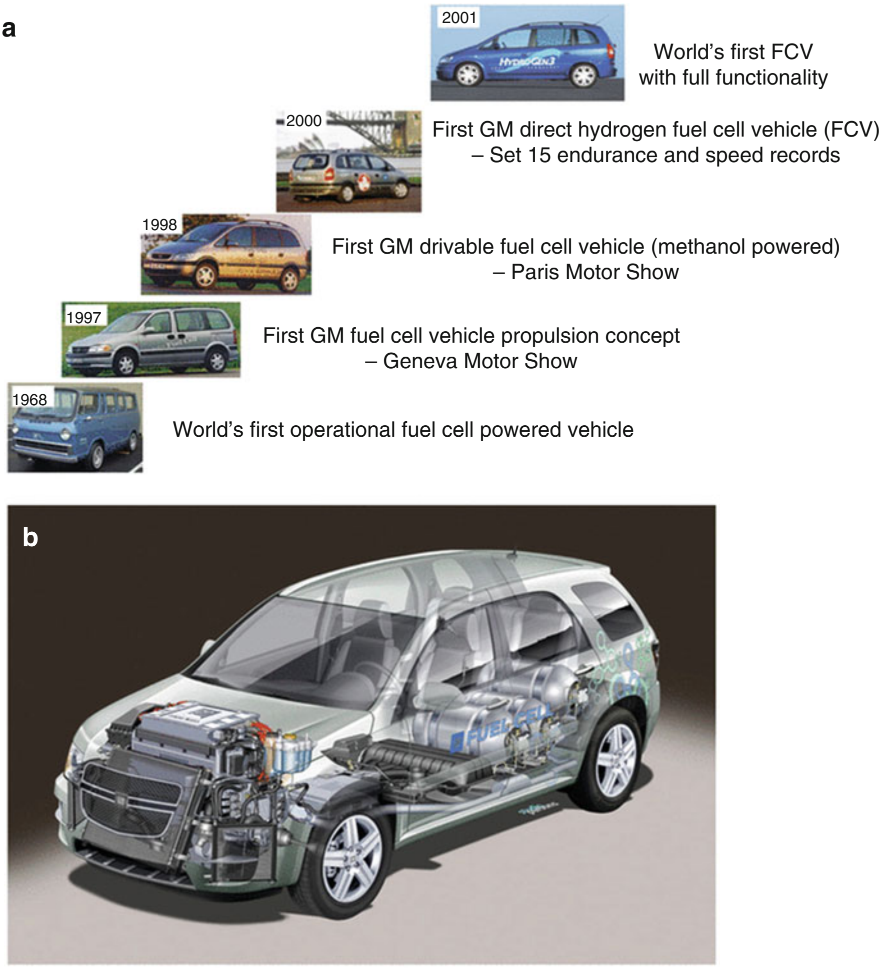

Polymer Electrolyte Membrane (PEM) Fuel Cells: Automotive Applications, Fig. 3 (**a**) Timeline of fuel cell vehicle development at General Motors until 2001; (**b**) 2008 Chevy Equinox fuel cell vehicle [24, 25]

torque, providing a range of 240 miles, and a refueling time of 3 min [27]. Ford Motor Company has also released a series of vehicles using Ballard stacks such as the P200HFC (1999), Focus FCV (2000), and Advanced Focus FCV (2002).

Toyota

Toyota has been developing fuel cells since about 1996 with vehicles such as the RAV 4 FCEV-hybrid (metal hydride, 1996), RAV 4 FCEV (methanol, 1997), FCHV-3 (metal hydride, 2001), FCHV-4 (compressed H_2, 2001), and FCHV-5 (reformed gasoline, 2001). Their efforts have resulted in the development of the latest Toyota Fuel-Cell Hybrid Vehicle (FCHV), some of which are being tested daily at the University of California in Davis and Irvine. Since 2001, a fleet of 25 FCHVs has accumulated more than 100,000 miles. In 2002, Toyota began limited marketing of the hydrogen-powered TOYOTA FCHV (fuel cell hybrid vehicle) in the USA and Japan [28]. Toyota FCHVs have also been successfully tested under subzero conditions. In real-world driving tests carried out in 2008 in collaboration with the US DOE, Savannah River National Laboratory, and National Renewable Energy Laboratory (NREL), the FCHV-adv averaged the equivalent of ~68 mpg achieving a range of ~430 miles on a single fill of compressed (70 MPa) hydrogen gas. Figure 6 depicts images

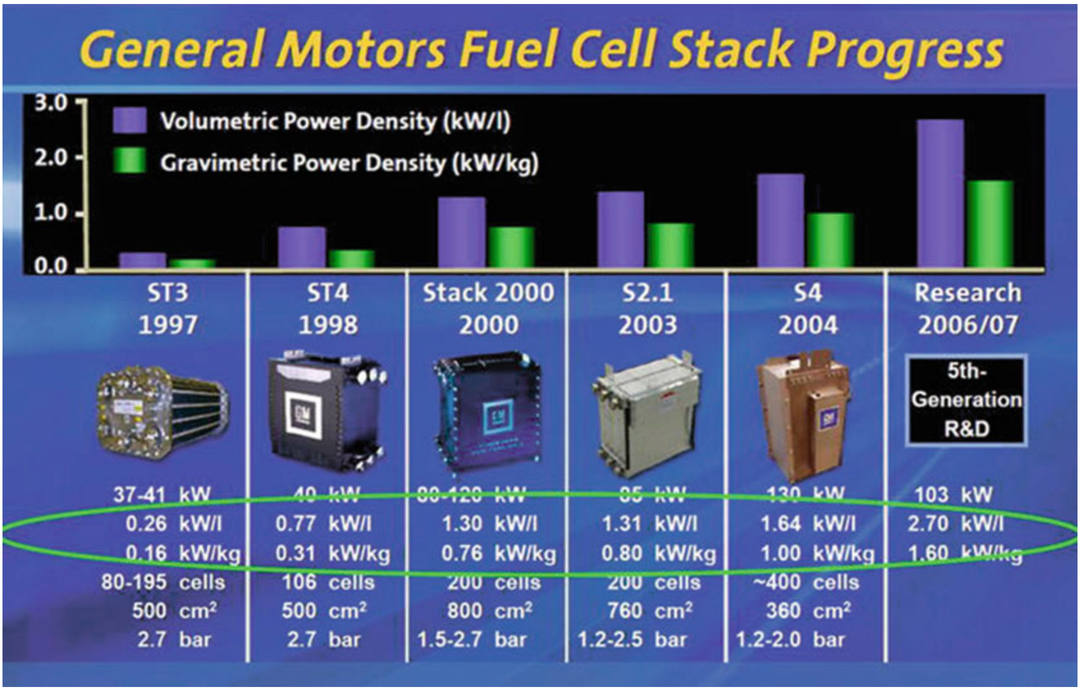

Polymer Electrolyte Membrane (PEM) Fuel Cells: Automotive Applications, Fig. 4 Advancements in the development of the fuel cell stacks designed at General Motors from 1997 to 2004 is depicted [22]

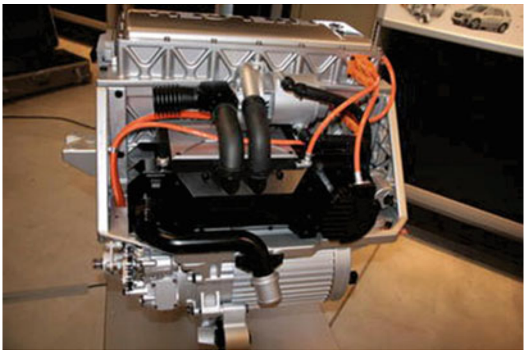

Polymer Electrolyte Membrane (PEM) Fuel Cells: Automotive Applications, Fig. 5 Photograph of fifth generation of General Motors PEMFC stack and system [23]

of Toyota's FCHV and an under the hood look at their PEMFC stack [29]. At this time (2017), Toyota has released a commercial FCEV the Toyota Mirai that can be purchased (~USD57,500) in Japan and California. The Toyota Mirai is now available for purchase for $57,500 with a 312 miles per fill, and 5 mins to refill. The fuel tank consists of a carbon fiber wrapped, polymer lined tank built to absorb five times the crash energy of steel. About 5 kg of hydrogen is stored at 70 MPa. The fuel consumption is rated at 67 mpge combined. The vehicle has a cold start capability of −30 °C. The vehicle is warranted for 8 years/100,000 miles on key components.

The key specifications are as follows:

Name	Toyota fuel cell stack
Fuel cell stack type	Solid polymer electrolyte fuel cell
Humidification system	Internal circulation system (humidifier-less)
Power output	153 HP (114 kW) MAX
Output density by volume	3.1 kW/L
Output density by weight	2.0 kW/kg
Cell number of cells in one stack	370 (single-line stacking)
Thickness	1.34 mm
Weight	102 g
Flow channel	3D fine-mesh flow field (cathode)
Emission rating	Zero emissions vehicle (ZEV)

Polymer Electrolyte Membrane (PEM) Fuel Cells: Automotive Applications,
Fig. 6 Images of Toyota's FCHV-adv installed with their PEMFC stack [29]

Motor type	AC synchronous electric generator
Power output	151 HP (113 kW) MAX
Peak torque	247 lb-ft (335 Nm)

Storage method	Carbon fiber reinforced tanks
Number of tanks	2

Nissan

Nissan's foray into the development of FCV technology started in 1996 in collaboration with various stack development partners such as Ballard and UTC Fuel Cells. In 1999, testing of a methanol-reforming fuel cell was initiated and in 2000 Nissan participated in the California Fuel-Cell Partnership (CaFP). Since 2004, Nissan has developed and used an in-house PEMFC stack in their FCVs. Their 2005 FCV employs 70 MPa hydrogen fuel tanks that allow the X-Trail FCV to have a driving range of about 300 miles. Figure 7 depicts the timeline for FCV development at Nissan along with metrics of driving range and acceleration time [30]. The range of their current generation vehicle is ~500 km (310 miles) and is comparable to a similar ICE powered vehicle. In 2007, they have developed a new generation of stacks that have significantly lower catalyst loadings, improved durability, high-rated power of 130 kW, and a volumetric power density approaching 2 kW/L. Specifications of Nissan's 2005 model FCV are detailed in Fig. 8.

Honda

A brief timeline for the development of FCVs by Honda is summarized below. Honda initially employed various 60–85 kW Ballard stacks in their initial FCVs such as the FCX-V1 (metal hydride, 1999), FCX-V2 (methanol, 1999), FCX-V3 (compressed H_2, 2000), FCX-V4 with ultra-capacitors (compressed H_2, 2001), and the FCX (compressed H_2, 2002) vehicle that was leased in Los Angeles.

The US City of Los Angeles became the first FCX customer, leasing the first of five Honda FCX models for fleet use. In 2003, a next-generation fuel cell stack capable of power generation at temperatures as low as −20 °C was announced. In 2005, Honda introduced the second-generation FCX and the first to be powered by a Honda FC stack. FCX Clarity FCEV, a dedicated platform hydrogen fuel cell vehicle, debuted at the LA Auto Show; the new stack was 20% smaller and 30% lighter than its previous generation. Since 2008, FCX Clarity FCEV has been made available as a leased vehicle for consumer use [31].

Some of the interesting aspects of the Honda fuel cell stack are the so-called V-Flow stack configuration that claims easy drainage of water, higher cell stability, aromatic electrolytic membrane, improved thermal management, and improved packaging. Honda has also reported the use of specialized coatings with impregnated electrical contacts on their bipolar plates that reduced the contact resistance while being corrosion resistant. Figure 9a depicts the conventional stack assembly and Fig. 9b and c illustrate their improved efficient stack packaging design. Honda has recently a commercially leasable FCEV, the 2018 Clarity (174 hp) that has a 366 mile EPA-range rating and can be refueled in 3–5 mins.

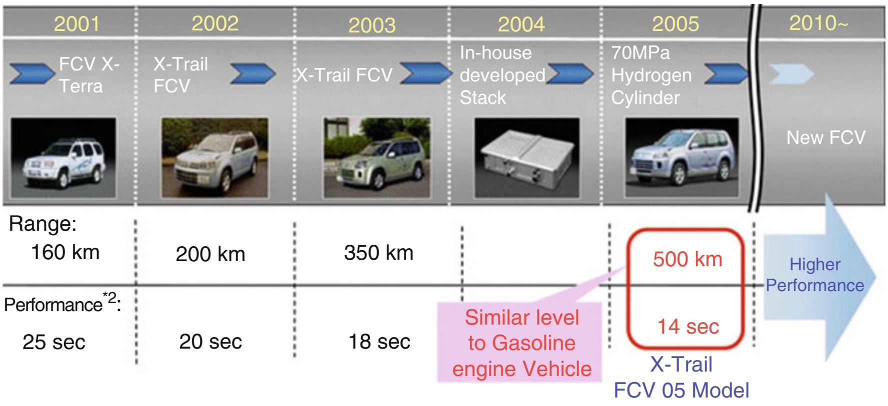

Polymer Electrolyte Membrane (PEM) Fuel Cells: Automotive Applications, Fig. 7 Timeline for FCV development at Nissan along with metrics of driving range and 0–100 kmph acceleration time [30]

The 2017 Honda Clarity is also available for commercial sale and has the following key specs:

Engineering	Clarity fuel cell
Proton electrolyte fuel cell (PEFC)	•
Operating range	−22 °F–221 °F
Power output	103 kW
Size	33 L
Weight	114 lbs
Lithium-ion battery	•
Output	346 volts
AC permanent-magnet synchronous electric motor	•
Horsepower (SAE net)	174 @ 4501–9028 rpm
Torque (SAE net)	221 lb-ft @ 0–3500 rpm
EPA mileage ratings[2]/fuel	Clarity fuel cell
5w?>Miles-per-gallon equivalent (MPGe), (city/highway/combined)	69 / 67 / 68
Driving range rating	366
Fuel tank capacity	5.46 kg
Fuel tank pressure	70 MPa / 10,000 psi
Required fuel	Compressed gaseous hydrogen

Automotive PEMFCS

In this section, the operational modes that fuel cell stacks are subjected to; the 2015 performance, cost, and durability targets that fuel cell technology must achieve; and recent advancements made by automotive companies toward achieving the targets for commercialization are discussed.

Operational Modes of Automotive PEMFCS

Unlike residential and stationary fuel cells, automotive PEMFCs undergo the entire slew of aggressive variable loads and environmental conditions that are typically experienced by conventional ICEs. The modes of operation of an automotive PEMFC can be simplified to the following [32]: (1) Idling/low load, (2) acceleration-deceleration/load cycling, (3) start-up shutdown, (4) cold temperatures/freeze-thaw cycles, and (5) contamination/impurities from the environments and cell degradation products. The impact of these modes of operation on the PEMFC stack is briefly discussed below. Unless otherwise specified, the discussion assumes a Pt nanoparticle-based electrocatalyst on a high-surface-area carbon black support, a perfluorosulfonic acid membrane, hydrogen flow on the anode, air flow on the cathode with the reactants partially humidified at the inlet. Testing is performed on a variety of platforms such as liquid electrolyte-half-cells (~0.198 cm^2), subscale fuel cells (25–50 cm^2), and full-size single cells or short stacks having active areas as high as 400 cm^2. The basic diagnostics techniques and characterization of fuel cell components can be found detailed in the literature [33–35].

Idling/Low Load

When a vehicle in operation is at rest, for example, at a stop light, the current drawn by the fuel cell stack is low; essentially power is drawn by the auxiliary equipment in the vehicle. At such low current densities, the cathode potential is high and may approach the open circuit voltage (OCV). Although the thermodynamic reversible potential at 80 °C is about 1.18 V, leakage currents (few mA/cm^2) especially due to hydrogen crossover across the (~20–50 μm thick) membrane and electronic shorting lower the OCV to about 0.95 V. This high cathode potential leads to several degradation phenomena in the cells. The Pt-based catalyst dissolves at these potentials and diffuses toward the anode through the membrane and within 48 h forms a band inside the membrane as shown in Fig. 10 [36]. This Pt band formed in the membrane induces chemical degradation of the membrane itself due to formation of OH, hydrogen peroxide, and peroxyl radicals resulting in membrane thinning. The chemical degradation is accelerated under low RH conditions and higher temperatures. Degradation of the membrane leads to an increase in hydrogen crossover and can result

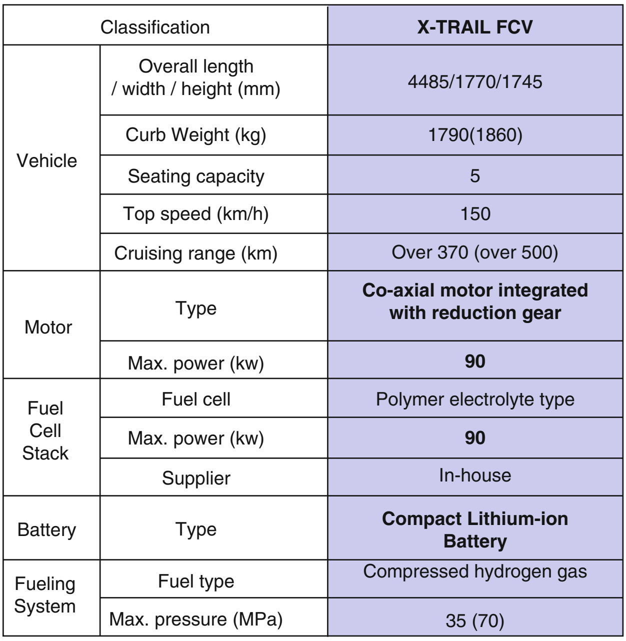

Classification		**X-TRAIL FCV**
Vehicle	Overall length / width / height (mm)	4485/1770/1745
	Curb Weight (kg)	1790(1860)
	Seating capacity	5
	Top speed (km/h)	150
	Cruising range (km)	Over 370 (over 500)
Motor	Type	**Co-axial motor integrated with reduction gear**
	Max. power (kw)	**90**
Fuel Cell Stack	Fuel cell	Polymer electrolyte type
	Max. power (kw)	**90**
	Supplier	In-house
Battery	Type	**Compact Lithium-ion Battery**
Fueling System	Fuel type	Compressed hydrogen gas
	Max. pressure (MPa)	35 (70)

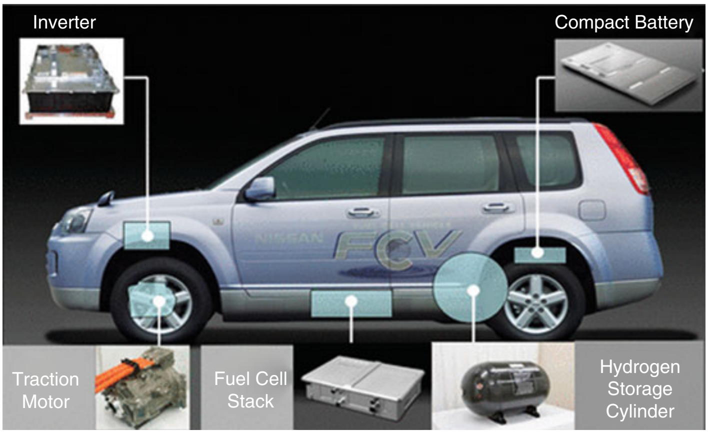

Fig. 8 (continued)

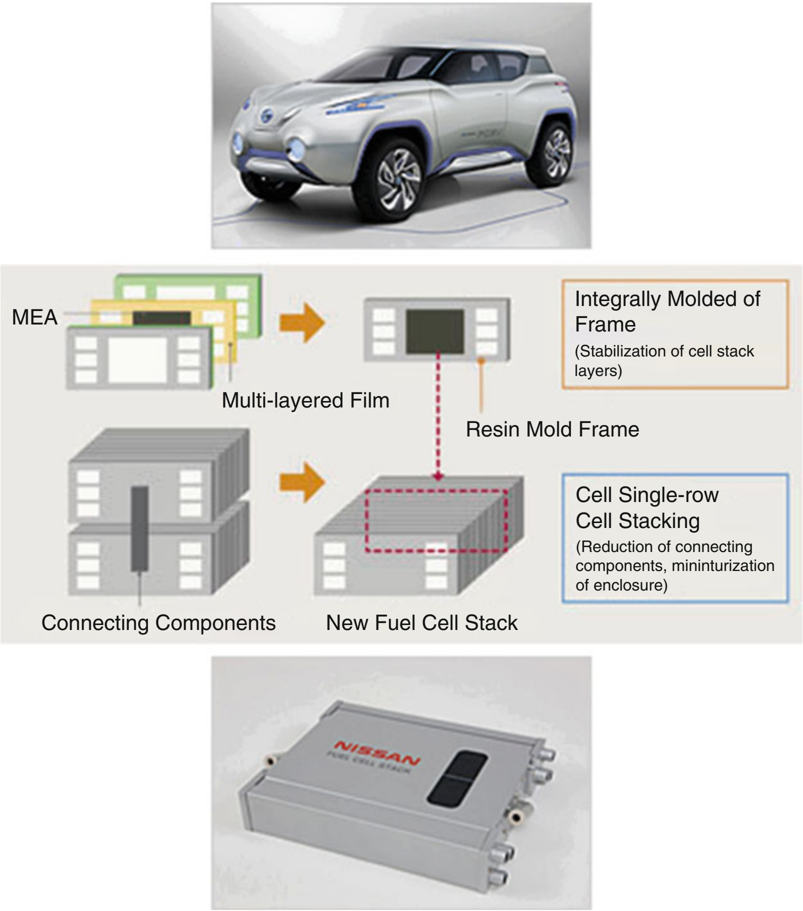

Polymer Electrolyte Membrane (PEM) Fuel Cells: Automotive Applications, Fig. 8 Detailed specifications of Nissan 2005 X-Trail FCV along with a layout of components of the fuel cell stack system. Next generation Nissan Terra SUV concept along with improvements to stack technology is also shown [30]

in thinning, pinholes, and eventually catastrophic failure. Figure 11 shows the fluoride and sulfate elution from the exhaust water of a fuel cell during and after OCV testing [37]. About 6% of the fluorine in the membrane is released during 48 h of OCV hold. If the carbon support (on which the catalyst is dispersed) has a high surface area and therefore susceptible to corrosion, it may first become hydrophilic and over time corrode and oxidize leading to some Pt nanoparticle agglomeration which also leads to cell performance loss. If the fuel cell is a hybrid with a 10–20 kW NiMH or Li-ion battery, it may be possible to minimize the deleterious effects of high cathode potentials by using appropriate system controls and algorithms to lower the high potentials.

Acceleration/Deceleration

PEMFC stacks in vehicles are subject to variable power demands that depend on environmental conditions such as the grade of the road as well as the driving behavior of the vehicle operator. As the load changes, the current drawn from the fuel cell and hence the cell voltage changes resulting in the cell being subject to load cycles or potential cycles. Thus, the fuel cell is subject to all kinds of potential cycles with the widest potential range being about 0.60–0.95 V [32, 35, 38–41]. The upper potential corresponds roughly to OCV/idling and the lowest potential corresponds to the potential at peak power (about 0.6 V and a few amperes per square centimeter). The upper limit of the voltage is determined by

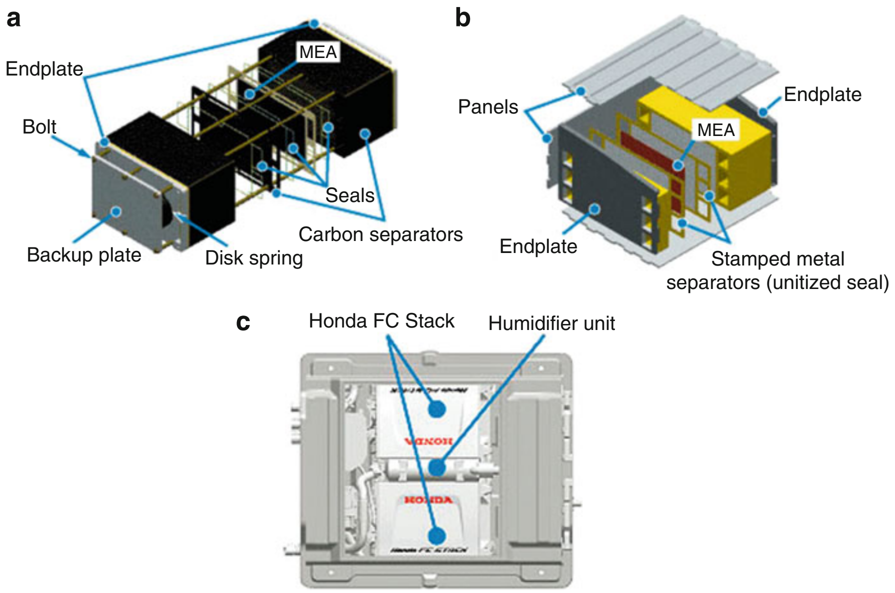

Polymer Electrolyte Membrane (PEM) Fuel Cells: Automotive Applications, Fig. 9 (**a**) Illustrates conventional stack package design of previous configurations and (**b**, **c**) illustrate Honda's new efficient stack package design [31]

the choice of the membrane (thickness/permeability) and in part by the design of the vehicle system controls. Although peak power is drawn from the stack for only ~5% of the time, it is necessary for the stack to have an electrical efficiency of ~55% (to be competitive with ICEs); also, the size of the stack is partly determined based on the peak power point.

A number of automotive drive cycles (FUDS cycle, US06, NEDC, and Japanese 10–15 mode drive cycles, etc.) are available to represent the statistical usage of a vehicle and are used to determine the mileage of ICE vehicles. Figure 12 is an example of the Japanese 10–15 drive cycle and Fig. 13 an example of the US06 drive cycle. These drive cycles can be systematically converted into voltage-time profiles and applied to estimate the degradations rates of stacks under simulated driving conditions. A generic individual cycle profile is shown in Fig. 14 that represents a superset of all possible profiles [32]. The five elements of the profile that can be varied are: (1) duration at low potential, (2) duration of the ramp-up from low to high potential (or ramp-up rate), (3) duration at high potential, (4) duration of the ramp-down from high to low potential (or ramp-down rate), and (5) duration at low potential. The high and low potentials can have infinitely different values between the upper and lower limit in the range 0.6–0.95 V.

It has been determined through a large number of studies that the widest potential cycles of 0.60–0.95 V cause the most degradation of the cathode catalyst layer. Automotives typically undergo 300,000 such cycles over their 5,000 h/10 years lifetime. At potentials above 0.95 V, the Pt surface is highly covered with oxide species while below 0.6 V it is almost free of oxide species as is observable from a typical cyclic voltammogram of platinum in acids or in a PEMFC. Thus, the process of cycling in the range 0.60–0.95 V results in the growth (oxidation) and stripping (reduction) of oxide species on the surface and prevents the formation of a stable passivating film. (A more conservative potential regime of 0.70–0.90 corresponding to the iRFree potential that the catalyst layer experiences is sometimes selected.) Figure 15 depicts both the enhanced activity of PtCo/C electrocatalysts over Pt/C [42] and the surface area

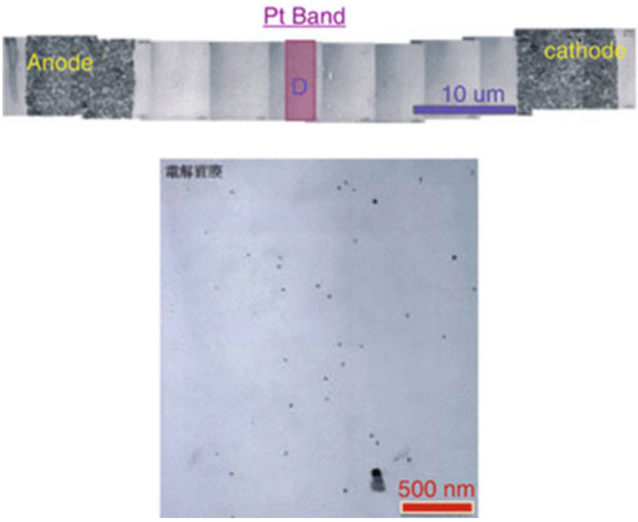

Polymer Electrolyte Membrane (PEM) Fuel Cells: Automotive Applications, Fig. 10 Formation of a Pt band (with magnified view of the band) in the membrane when held under OCV conditions over a period of 100 h [36]

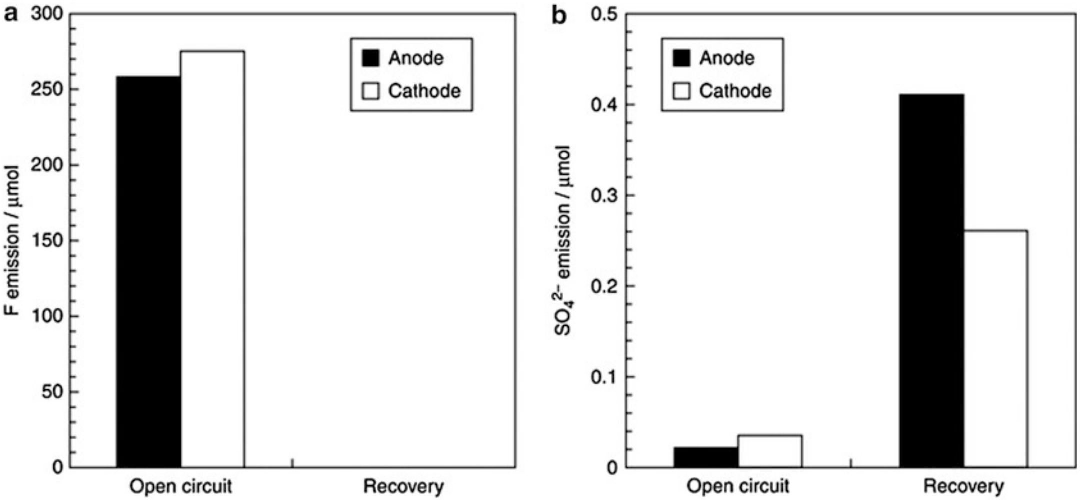

Polymer Electrolyte Membrane (PEM) Fuel Cells: Automotive Applications, Fig. 11 Fluoride emission during OCV hold test (6% of fluorine in the membrane is released over a 48 h hold) and sulfate emissions during recovery operation [37]

loss during cycling [39]. Based on recent research, it appears that exposure of bare (oxide-free) Pt to high potentials during the anodic portion of a scan in a cycle has a high impact on the Pt dissolution and degradation of the cathode catalyst layer. Again, practical methods that involve limiting the number of large cycles with the help of a battery in a hybridized system mitigate the losses partially. Pt-based alloys, heat-treated Pt, and other modifications to the catalyst layer also provide partial material solutions that restrict the losses.

Start-Up/Shutdown

Automotive PEMFC stacks are shut down and started a number of times depending on the needs of the driver; the number of such occurrences is about ~30,000 over the stack life. When an automotive PEMFC stack is allowed to rest for a period of time, both the anode and

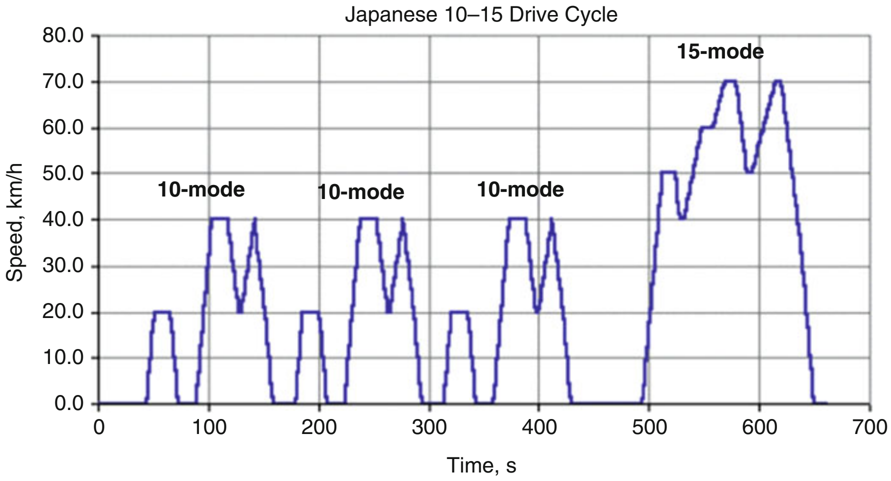

Polymer Electrolyte Membrane (PEM) Fuel Cells: Automotive Applications, Fig. 12 Japanese 10–15 drive cycle for automobiles

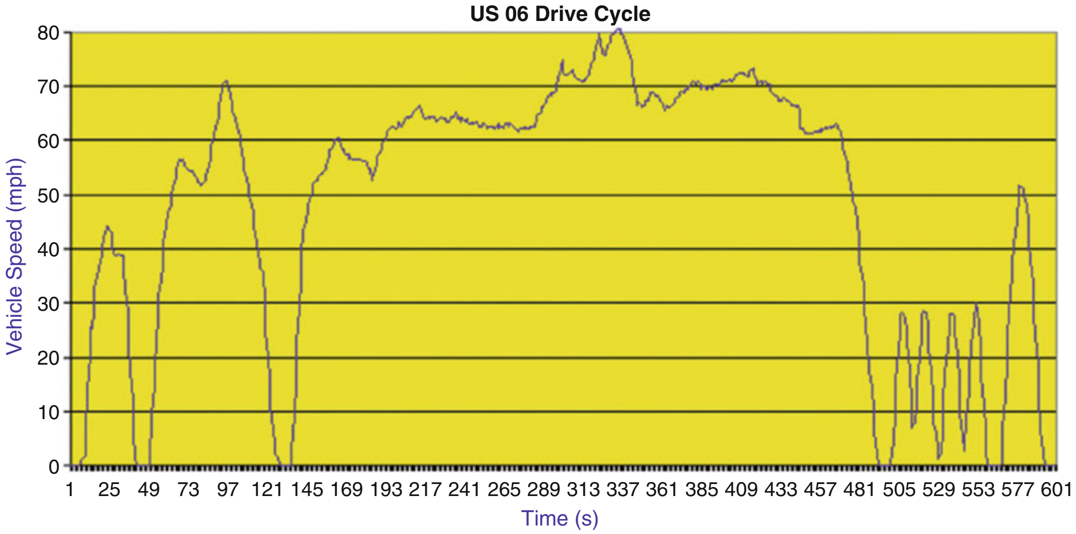

Polymer Electrolyte Membrane (PEM) Fuel Cells: Automotive Applications, Fig. 13 US 06 drive cycle for automobiles

cathode chambers get filled with ambient air from the atmosphere. When such a stack filled with air is restarted and hydrogen turned on to flow on the anode side, it pushes out the air leading to the formation of a "H_2-air front." It was discovered around 2001 that frequent starting and shutting down of fuel cells resulted in a peculiar phenomenon where the cathode becomes subject to potential transients as high as 1.5 V [43–45]. At these high potentials, the carbon support of the cathode catalyst layer undergoes precipitous corrosion to carbon dioxide. Loss of the carbon leads to agglomeration of the Pt nanoparticles resulting in a loss in catalyst surface area, severe mass-transport issues, and a precipitous loss in cell performance. No losses are observed if the start-up takes place within a short time of shutdown as long as there is residual hydrogen in the anode of the fuel cell; thus the time interval between start-up and shutdown is an important parameter governing overall degradation rate [46].

Figure 16 below is a schematic of the start-up/shutdown phenomenon and the reactions that occur in the anode and cathode catalyst layers. Interestingly, no damage occurs on the anode-side catalyst layer. Figure 17 depicts the degraded cross section of an MEA (cathode facing up) after ~50 start-up/shutdown cycles. Over the last decade, several mitigation techniques that involve controlling the procedure at start-up and shutdown have been reported and losses have been minimized, albeit at the expense of system complexity. Some of the mitigating solutions include: (1) shorting the stack to minimize the potential spike, (2) purging the anode using high flows of gases to minimize the H_2-air front time (to less than 0.5 s), (3) drying the stack after shutdown, (4) lowering the Pt loading on the anode side to lower the ORR with a consequent suppression of the COR on the cathode, and (5) lengthening the time for which residual hydrogen remains in the anode, etc. The search for more durable corrosion-resistant supports to replace carbon is underway so that the fuel cell system can be simplified. Oxides, nitrides, carbides, of tungsten, titanium, etc., are promising candidates but they often suffer from poor electronic conductivity, lower surface area compared to carbon blacks, and it can be difficult to disperse Pt nanoparticles on them [47].

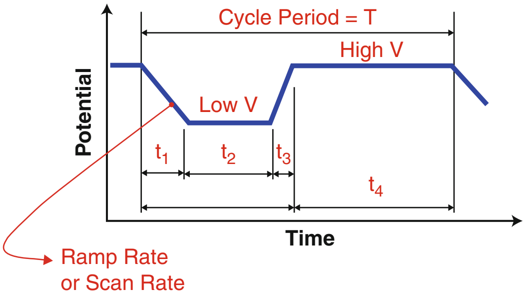

Polymer Electrolyte Membrane (PEM) Fuel Cells: Automotive Applications, Fig. 14 Schematic representation of an arbitrary cycle extracted from a complex drive cycle illustrating the various parameters that can be varied in the cycle profile

Cold Temperatures

Automotive PEMFCs must be capable of enduring cold weather conditions such as freezing temperatures as low as −40 °C. Even conventional ICE vehicles need help from engine block warmers, etc., in order to be able to start-up from subzero conditions. Under subzero conditions, an operating fuel cell will generate sufficient heat to prevent water from freezing and will likely show

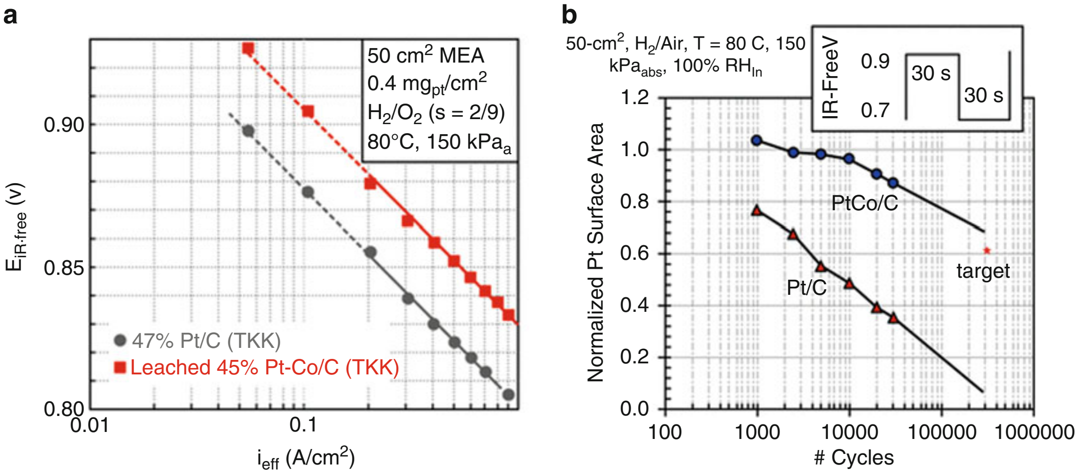

Polymer Electrolyte Membrane (PEM) Fuel Cells: Automotive Applications, Fig. 15 (**a**) Enhanced activity (×3) under $H_2|O_2$ for pre-leached PtCo/C electrocatalysts compared to Pt/C as tested in subscale fuel cells [42]; (**b**) electrochemical area loss for Pt/C versus PtCo/C catalysts over 10,000 cycles in subscale fuel cells illustrates lower degradation for the PtCo/C [39]

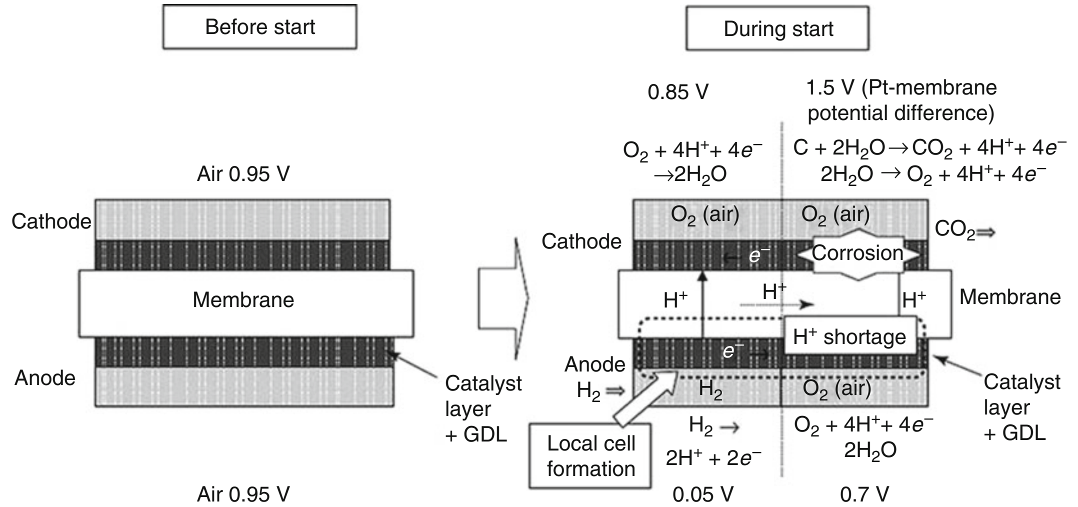

Polymer Electrolyte Membrane (PEM) Fuel Cells: Automotive Applications, Fig. 16 Schematic of start-up/shutdown phenomenon before and during passage of the H_2-Air front through the anode chamber [43–46]

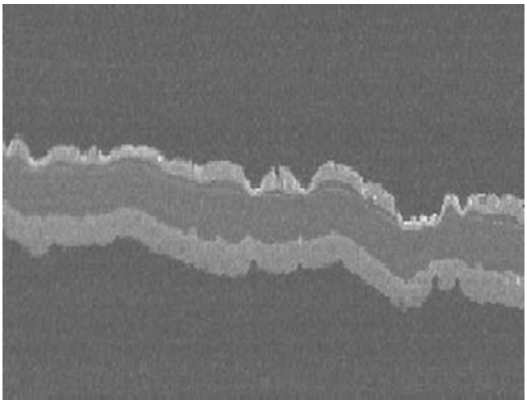

Polymer Electrolyte Membrane (PEM) Fuel Cells: Automotive Applications, Fig. 17 SEM cross section of an MEA with the cathode (top) layer showing severe corrosion and degradation after about 50 uncontrolled start-up/shutdown cycles. A light band is also observed near the cathode-membrane interface due to the cycling of potential that takes place between 1 and 1.5 V

little or no loss in performance. The problem arises when a PEMFC has been idle for a long period of time under subzero conditions and is required to start-up.

PEMFCs have the added challenge of liquid water in the system that can freeze, block channels and gas flow paths, and form icicles that may penetrate through the polymer membrane and cause damage. Blockage of channels can lead to fuel starvation, carbon corrosion, and degradation of the anode/cathode catalyst layer. The use of insulation, heaters, and antifreeze coolants are helpful for short periods of time, but the residual water within the fuel cell will eventually freeze forming ice. The catalyst layer and the diffusion media are especially susceptible to repeated freeze-thaw cycles due to their porous nature and the inherent presence of water (loosely bound and free water) that can expand and contract leading to a disruption of the porous structure that is so important for mass transport. Significant disconnection of the catalyst particles from the ionomer and carbon support could result in degradation in performance due to the loss in protonic and electronic interfacial contact.

Elimination or minimization of the water in the cells by purging with gases or vacuum drying prior to shutting down the stack is a general approach that has been found to be effective. In short, “keeping the stack warm” and “removal of water” are essentially the two main strategies to counter the cold start issue. The principal targets that automotive PEMFC stacks are required to meet are the ability to start unassisted from −40 °C and a cold start-up time to 50% of rated power in 30 s (from −20 °C) with a start-up energy consumption of <5 MJ [48]. Most automotive manufacturers have claimed to have achieved the targets although research to understand the phenomenon in detail continues.

Contamination/Impurities

PEMFCs are very clean systems and act as filters for impurities introduced from ambient air, fuel used, and even degradation products from the cell materials. Both the membrane and the catalyst are susceptible to contamination and poisoning. Electrode degradation of PEMFCs can occur as a result of various impurities found in the fuel feed, air stream, as well as corrosion by-products from fuel cell components such as the bipolar plate, catalysts, or membrane.

Hydrogen for PEMFCs can come from various sources including reformed fossil fuels. Therefore, depending on the reforming technique and degree of posttreatment, small amounts of contaminants such as CO, CO_2, NH_3, and H_2S are expected to be present in the fuel stream [49]. Trade-offs in the level of impurities are unavoidable since ultrahigh purification would lead to elevated costs of hydrogen. The US FreedomCAR technology team has arrived at preliminary fuel mixture specifications that include: >99.9% H_2, 10 ppb H_2S, 0.1 ppm CO, 5 ppm CO_2, and 1 ppm NH_3. Hydrocarbons such as methane, benzene, and toluene are other common impurity by-products from reforming processes.

Atmospheric air contains 78% nitrogen and 20% oxygen with the remainder being a number of trace gases and particulates depending on the local air quality. Pollutants found in the atmosphere include nitrogen oxides (NO and NO_x), hydrocarbons, carbon monoxide (CO), ozone, sulfur dioxide (SO_2), fine primary and secondary particulate matter, and chloride salts from the ocean and deicers. Chloride anions adsorb on Pt, occupy reaction sites, and significantly lower the ORR activity; fortuitously, the loss is recoverable simply by flushing out the anions with generated water. The degradation of performance due to 2.5 and 5 ppm SO_2 in the air stream was reported to be about 50% and 80%, respectively, by Mohtadi et al. [50]. The degradation is due to chemisorption of sulfur species on the Pt catalyst, and oxidation by the application of high potentials (CV) reversed the degradation but operation under normal potentials did not [51]. The poisoning mechanism by NO_2 was reported to be dependent on the time of exposure rather than bulk concentration and could apparently be reversed by operation under clean air for 24 h. Figure 18 depicts the loss in performance of a subscale fuel cell as a result of contamination of the catalyst in the presence of SO_2, H_2S, NO, NO_2, and NH_3 [51]. The PEM is also easily contaminated by cationic impurities that may enter the stack through water, dissolved catalyst cations [52], as well as corrosion products from the bipolar plate. The loss in cell performance is fairly severe due to the lowering of the conductivity of the membrane.

The Status and Targets for Automotive PEMFC Commercialization

The overall status and targets for automotive PEMFC systems as well as hydrogen production, delivery, and storage are outlined in Table 1. All of the targets need to be attained for successful commercialization of fuel cell vehicles.

The performance, durability, and cost of PEMFC system and stacks for automotives are approaching levels such that major automotive manufacturers have projected that commercialization will commence around 2015. The US DOE has had cost analysis conducted by independent organizations and estimates assuming 500,000 units/year indicate that system cost has been lowered from $275/kW in 2002 to $73/kW in 2008 [53, 54]. The target for PEMFC system cost in 2015 is $30/kW. The durability of stacks under automotive conditions is currently around 2,500–3,000 h with the target in 2015 being 5,000 h.

In order to achieve commercialization in 2015, the targets of performance, durability, and cost of the fuel cell components (catalyst, membrane, diffusion media, bipolar plates, etc.,) and the system (thermal, fuel, air, and water management, and balance of plant) have to be met simultaneously. For example, high durability can easily be achieved by utilizing high loadings of Pt catalyst, corrosion-resistant bipolar plates with expensive coatings, etc., but this would violate the cost targets. It is required to maintain the performance of PEMFC stacks of today while at the same time lower the precious metal catalyst loadings by a

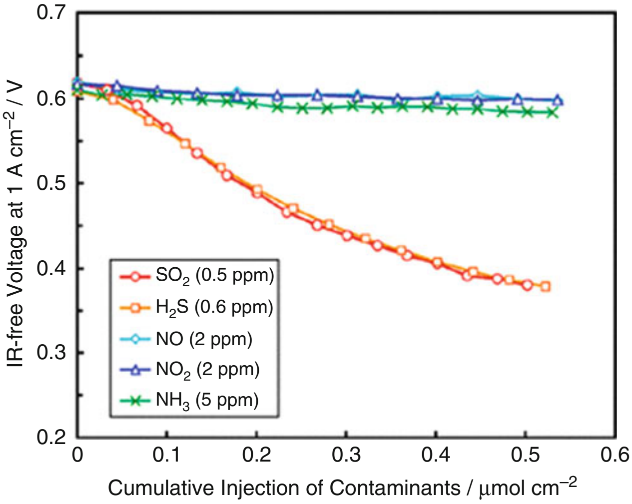

Polymer Electrolyte Membrane (PEM) Fuel Cells: Automotive Applications, Fig. 18 The impact of several air contaminants on a fuel cell operated at 1 A/cm^2 [51]

Polymer Electrolyte Membrane (PEM) Fuel Cells: Automotive Applications, Table 1 Overall status and targets for PEMFC systems, hydrogen storage, production, and delivery [48]

	Status	Target
Fuel cell system cost	\$61/kW	\$30/kW
Fuel cell system durability	2,000–3,000 h	5,000 h
Hydrogen production	\$3–\$12/gge	\$2–\$3/gge
Hydrogen delivery	\$2.30–\$3.30/gge	\$1/gge
Hydrogen storage gravimetric	3.0–6.5 wt.%	7.5 wt.%
Hydrogen storage volumetric	15–50 g/L	70 g/L
Hydrogen storage cost	\$15–\$23/kWh	\$2/kWh

factor of 4–10 and increase the stack durability by a factor of ~2.

Basis for Targets

The targets of performance and durability of PEMFC stacks are loosely based on that of IC engines used in automotives today. Durability targets are being addressed by organizations such as the US DOE's Office of Energy Efficiency and Renewable Energy's Hydrogen Fuel Cells and Infrastructure (HFCIT) program in close association with national laboratories, universities, and industry [48], the New Energy and Industrial Technology Development Organization (NEDO) in Japan [55], and the European Hydrogen and Fuel Cell Technology Platform (HFP) and Implementation Panel (IP) in Europe. The Fuel Cell Commercialization Conference of Japan (FCCJ) has also published a booklet defining performance, durability, and cost targets in collaboration with Nissan, Toyota, and Honda and a summary has been reported elsewhere [56]. Overall, the general 2015 target for fuel cell stack durability (in cars) is roughly defined to be 5,000 h (150,000 driven miles) at the end of which ~10% performance degradation is allowable. This includes ~30,000 cycles of start-up/shutdown, ~300,000 cycles of wide span load, and hours of idling. So far ~3,000 h of stack life with low degradation rates has been demonstrated and steady progress is being made toward the final goal. An additional durability enhancement by a factor of <2× is needed for attaining the commercialization targets of 2015.

The cost breakdown of PEMFC systems is as illustrated in Fig. 19: The most expensive component (22% of system cost) is the precious metal (~\$40/g$_{Pt}$) catalyst used on the anode and cathode of each cell. Figure 20 shows the estimated reduction in cost of PEMFC stack system that has been achieved between 2002 and 2009. Figure 21 charts the breakdown of cost by subsystem and component for automotive PEMFC stacks.

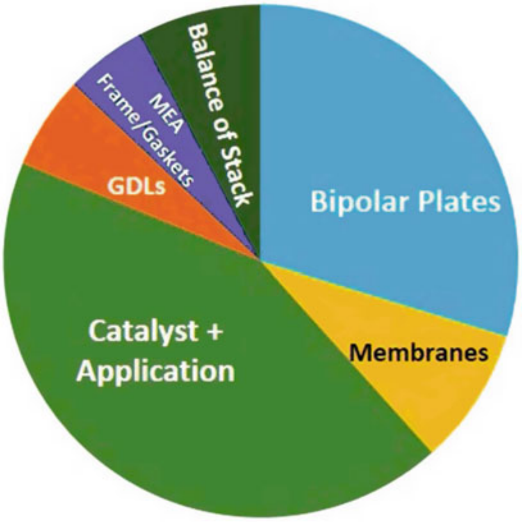

Polymer Electrolyte Membrane (PEM) Fuel Cells: Automotive Applications, Fig. 19 Cost structure for automotive PEMFC stack system [53, 54]

Electrocatalyst Targets The amount of Pt currently being used in ultra low emission IC engine automobiles (Pt, Pd, Rh, etc.) used in automotive catalytic converters can be as high as 6–10 g. This provides a justification for limiting the amount of Pt in a stack to ~10 g (in a typical 100 kW stack) or ~0.1 g_{Pt}/kW. Recycling of Pt used in fuel cells has been evaluated extensively by Tiax and the conclusion is that more than 90% of the Pt in fuel cell stacks is recyclable. Table 2 outlines the latest targets for automotive PEMFC electrocatalyst activity and costs.

Membrane Targets Today's membranes show excellent protonic conductivity (~100 mS/cm) at 100% RH and temperatures below 80 °C. PFSA membranes have been improved over the last few years to also achieve durability values that are approaching the target values of 5,000 h. These improvements involve modification of PFSA membranes by varying the casting conditions, thermal pretreatments, forming composites, employing reinforcements, using different lengths of pendant side chains, fluorinating the end groups, etc. In particular, micro-reinforced membranes (such as those from W. L. Gore [57]) allow for the use of thinner membranes that result in the use of less ionomer, improve the back diffusion of water, lower the protonic resistance, and generally result in higher power density fuel cells.

For automotive operation, it would be helpful to have a membrane material that could function with high proton conductivity at a low RH and higher temperatures. It would allow for simplified humidification systems and improved heat rejection (smaller radiator) and improved cell performance (mass transport) is expected due to the absence of liquid water. Membranes that exhibit sufficient conductivity at high temperature by retaining water necessitate the use of higher stack pressures (and higher parasitic compressor-related losses) especially as the temperature exceeds the boiling point of water at ambient pressure.

A cheaper hydrocarbon membrane is also desirable. Hydrocarbon membranes prepared from aromatic block copolymers constituted of alternating rigid sulfonic acid segments with hydrophobic polymeric units that are flexible have been reported. The unique morphology of the membrane provides comparable chemical stability as PFSA commercial membranes with high durability and a wide operating temperature range. Such membranes are already being used by automakers such as Honda. Other hydrocarbon-based membranes that are being actively researched include the use of di-sulfonated poly (arylene ether) sequenced block and random copolymers [58].

The key requirements for survivability and durability of membranes used in PEMFCs are mechanical durability (RH cycling, subzero start-up, shorting) and chemical durability (OCV holds). Survivability refers to the ability of the membrane to withstand operating conditions without the formation of pinholes that would lead to catastrophic hydrogen crossover and stack failure. Under subzero conditions, membranes can fail if the stack is not designed to eliminate most of the water in the flow fields to prevent formation of ice that can penetrate and damage the membrane on start-up. Durability refers to the slow thinning of the membrane over thousands of hours resulting in increased hydrogen crossover, membrane thinning, and

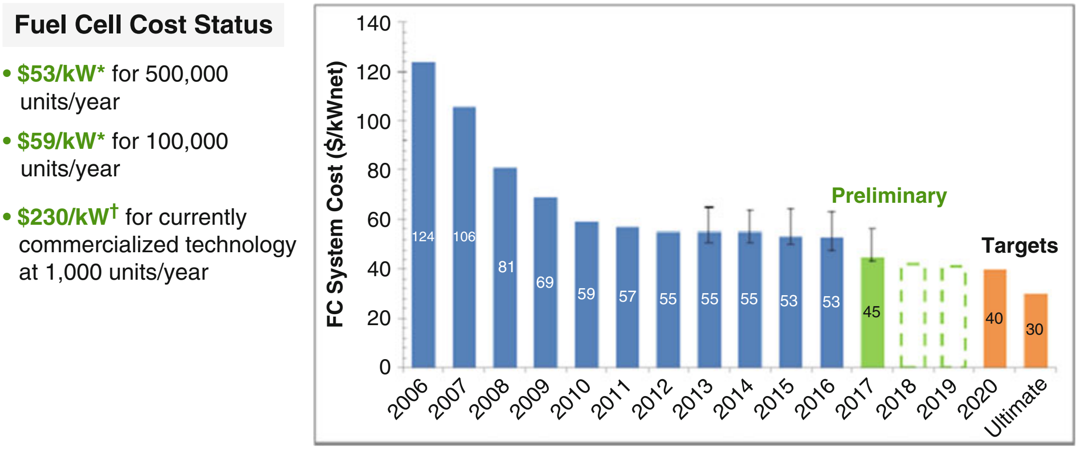

Polymer Electrolyte Membrane (PEM) Fuel Cells: Automotive Applications, Fig. 20 Reduction in cost of PEMFC stack system since 2002 and projected values and target for 2010 and 2015 [53]

Polymer Electrolyte Membrane (PEM) Fuel Cells: Automotive Applications, Fig. 21 Sensitivity of cost by subsystem and component for automotive PEMFC stacks [53]

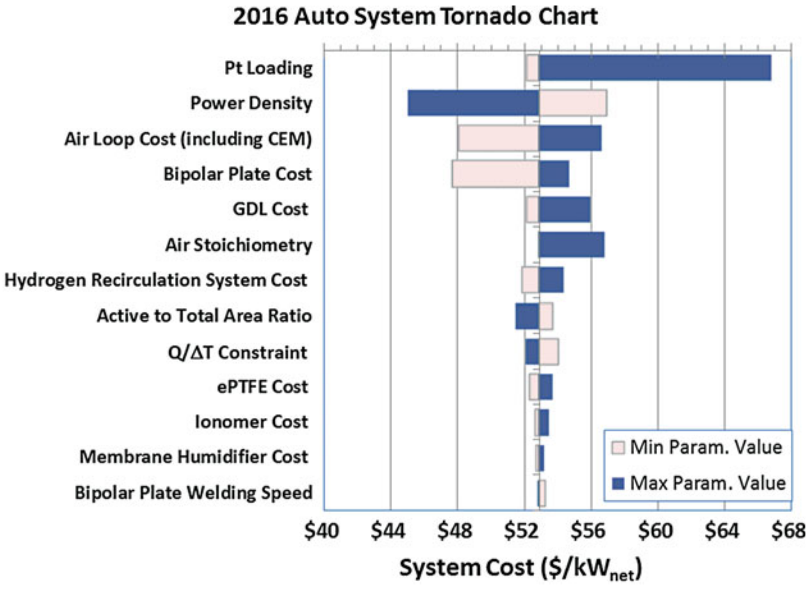

consequent loss of cell performance. The membrane (restrained in a cell) is mechanically stressed (fatigue) when the fuel cell RH cycles between dry and wet conditions; thermal cycles also play a role. In the laboratory, tests have shown that nonreinforced PFSA membranes fail in a few hundred hours or ~6,000 cycles while reinforced membranes last as long as 1,000 h or 60,000 cycles. Shorting is a mechanical degradation leading to electronic leakage currents through the membrane that may occur due to overcompression or penetrating irregularities from the catalyst layer or fibers of the diffusion medium. Shorting failures can be partially mitigated by using lower compression pressures (typically ~1,200 kPa), applying a coating of carbon black-based microporous layer (MPL) on the diffusion medium, etc. Chemical degradation of membranes is accelerated under OCV conditions where the potential is high and no water generated, as well as under generally low RH operation.

Polymer Electrolyte Membrane (PEM) Fuel Cells: Automotive Applications, Table 2 Targets for automotive PEMFC electrocatalyst activity and costs. Mass Activity @ 0.90 V, $H_2|O_2$, 80 °C, P_{H2}, P_{O2} = 100 kPa (based on multiple sources)

Characteristic	Units	2015 Status	2020 Targets
Platinum group metal total content (both electrodes)[a]	g/kW (rated,[b] gross) @ 150 kPa	0.16[c,d]	0.125
Platinum group metal (pgm) total loading (both electrodes)[a]	mg PGM/cm^2 electrode area	0.13[c]	0.125
Mass activity[e]	A/mg PGM @ 900 $mV_{iR\text{-}free}$	>0.5[f]	0.44
Loss in initial catalytic activity[e]	% mass activity loss	66[c]	<40
Loss in performance at 0.8 A/cm^2[e]	mV	13[c]	<30
Electrocatalyst support stability[g]	% mass activity loss	41[h]	<40
Loss in performance at 1.5 A/cm^2[g]	mV	65[h]	<30
PGM-free catalyst activity	A/cm^2 @ 0.9 $V_{IR\text{-}free}$	0.016[i]	>0.044[j]

[a] PGM content and loading targets may have to be lower to achieve system cost targets

[b] Rated power operating point depends on MEA temperature and is defined as the voltage at which $V = 77.6/(22.1 + T\ [°C])$, based on target of $Q/\Delta Ti = 1.45$ kW/°C and definition of $Q/\Delta Ti$ from Table 3.4.4, with an approximation of MEA temperature as equal to stack coolant outlet temperature

[c] Steinbach et al. (3 M), "High-Performance, Durable, Low-Cost Membrane Electrode Assemblies for Transportation Applications," 2014 Annual Merit Review, http://www.hydrogen.energy/gov/pdfs/review14/fc104_steinbach_2014_o.pdf

[d] Based on MEA gross power at 150 kPa abs. Measured at 0.692 V and 90 °C, satisfying $Q/\Delta T < 1.45$ kW/°C. At 250 kPa abs status is 0.12 g/kW

[e] Measured using protocol in Table P.1

[f] Kongkanand et al. (General Motors). "High-Activity Dealloyed Catalysts," 2014 Annual Merit Review, http://www.hydrogen.energy.gov/pdfs/review14/fc087_kongkanand_2014_o.pdf

[g] Measured using protocol in Table P.2

[h] B Popov et al. "Development of Ultra-low Doped-Pt Cathode Catalysts for PEM Fuel Cells," 2015 Annual Merit Review, http://www.hydrogen.energy.gov/pdfs/review15/fc088_popov_2015_o.pdf

[i] P. Zelenay (LANL). "Non-Precious Metal Fuel Cell Cathodes: Catalyst Development and Electrode Structure Design," 2016 Annual Merit Review, https://www.hydrogen.energy.gov/pdfs/review16/fc107_zelenay_2016_o.pdf

[j] Target is equivalent to PGM catalyst mass activity target of 0.44 A/mg_{PGM} at 0.1 mg_{PGM}/cm^2

Chemical degradation of the membrane is measured in terms of the fluoride release rate (FRR in g $F^-/cm^2\dot{c}h$) in the collected water; the FRR exhibits Arrhenius dependence with temperature in the range 50–120 °C. The FRR is of the order of 1.0×10^{-5} for typical membranes tested under OCV conditions and has been lowered with newer membranes to 1.0×10^{-7}. It should be noted that the mechanism of membrane degradation is not fully understood and is an area of intensive research. The two commonly invoked mechanisms are based on the assumption that hydrogen peroxide formed in the catalyst layer or at the Pt band in the membrane forms a hydroxyl radical which decomposes the membrane/ionomer by unzipping the less stable end groups or by scission of the main polymer chain. In actuality, mechanical and chemical degradation occur simultaneously in fuel cells accelerating the failure of the membrane.

The targets for membrane performance and durability based on figures reported by Nissan, USDOE, and the FCCJ are very similar. In order to be able to design a system that can reject heat at peak power, the fuel cell stack needs to operate for short spurts of time at temperatures as high as 90–95 °C. At this time, most fuel cell stacks operate at about 80 °C due to the restrictions of system complexity, parasitic (compressor) losses, and humidification requirements. The membrane is targeted to operate at temperatures above 100 °C (preferably 120 °C) at RH <30% while exhibiting a membrane conductivity of >100 mS/cm. The durability targets are similar to that for the complete fuel cell and includes <10%

performance loss over 5,000 h/10 years of operation under automotive conditions that includestart-up/shutdown, load cycling, freeze (−40 °C), and idling. The target cost of the membrane is \$10–20/m^2 for production levels of 10 million m^2/year. More detailed membrane performance targets base on USDOE and other sources are detailed in Table 3.

Bipolar Plate Targets Graphite bipolar plates have been used for a long time and are still being used in some fuel cell stacks. Graphite has a very high electronic conductivity, low interfacial contact resistance (ICR), and high corrosion resistance. Disadvantages of graphite bipolar plates are the high cost of material and machining, increased stack volume, high gas permeability, etc., although high volume manufacturability is somewhat better with polymer-carbon fiber and composite bipolar plates. Graphite-polymer composite plates have also been researched to improve the manufacturability of graphite plates while maintaining conductivity and stability with temperature. Bare metal plates do not have the disadvantages mentioned above but suffer from high ICR and poor corrosion resistance that can lead to metal dissolution and possible poisoning of the

Polymer Electrolyte Membrane (PEM) Fuel Cells: Automotive Applications, Table 3 Targets for selected properties of automotive PEMFC membranes [48]

Characteristic	Units	2015 Status	2020 Targets
Maximum oxygen crossover[a]	mA/cm^2	2.4[b]	2
Maximum hydrogen crossover[a]	mA/cm^2	1.1[c]	2
Area specific proton resistance at:			
Maximum operating temperature and water partial pressures from 40–80 kPa	ohm cm^2	0.072 (120 °C, 40 kPa)[c]	0.02
80 °C and water partial pressures from 25–45 kPa	ohm cm^2	0.027 (25 kPa)[c]	0.02
30 °C and water partial pressures up to 4 kPa	ohm cm^2	0.027 (4 kPa)[c]	0.03
−20 °C	ohm cm^2	0.1[b]	0.2
Maximum operating temperature	°C	120[c]	120
Minimum electrical resistance	ohm cm^2	>5,600[c]	1000
Cost[d]	\$/m^2	17[e]	20
Durability[f]			
Mechanical	Cycles until >15 mA/cm^2 H_2 crossover[g]	23,000[c]	20,000
Chemical	Hours until >15 mA/cm^2 crossover or >20% loss in OCV	742[c]	>500
Combined chemical/mechanical	Cycles until >15 mA/cm^2 crossover or >20% loss in OCV	–	20,000

[a] Tested in MEA on O_2 or H_2, 80 °C, fully humidified gases, 1 atm total pressure. For H_2 test methods, see M. Inaba et al. Electrochimica Acta, 51, 5746, 2006. For O_2 test methods, see Zhang et al. Journal of the Electrochemical Society, 160, F661–F622, 2013

[b] 14 µm PFIA membrane with nanofiber support. M. Yandrasits (3 M), private communication, February 1, 2016

[c] Reinforced and chemically stabilized PFIA membrane. M. Yandrasits et al. (3 M), U.S. Department of Energy Hydrogen and Fuel Cells Program 2015 Annual Progress Report, https:www.hydrogen.energy.gov/pdfs/progress15/v_b_1_yandrasits_2015.pdf

[d] Costs projected to high-volume production (500,000 80 kW systems per year)

[e] Cost when producing membrane for 500,000 systems per year. DOE Hydrogen and Fuel Cells Program Record 15,015, “Fuel Cell System Cost – 2015.” http://www.hydrogen.energy.gov/program_records.html

[f] Measured according to protocols in Table P.3, Table P.4, and Table P.5

[g] For air or N_2 testing, an equivalent crossover metric of 0.1 sccm/cm^2 at a 50 kPa pressure differential, 80 °C, and 100% RH may be used as an alternative

PEMFC stack components. The dissolved metal ions can contaminate/lower the conductivity of the membrane by taking up ion exchange sites or adsorb on the catalyst and lower its activity. The stacks are generally tolerant to about 5–10 ppm of metal ion contamination. At the compression forces of relevance to PEMFCs, the USDOE bipolar plate areal resistivity target for ICR is 10 mΩ-cm^2.

Stainless steels, as well as Al-, Ni-, and Ti-based alloys, have been studied extensively as possible candidates for bipolar plates. One of the most well-studied materials for bipolar plates is SS 316/316 L (16–18% Cr, 10–14% Ni, 2% Mo, rest Fe); other candidates are 310,904 L, 446, and 2205. Bare stainless steel plates form a passive 2–4 nm chromium oxide surface layer under PEMFC conditions that leads to unacceptably high ICRs. A similar trend is observed for the other alloys and therefore surface modification or surface coatings on selected substrate material has to be considered as a pathway to meet the technical targets of low ICR and high corrosion resistance.

Coatings may be metal based, such as gold, TiN, CrN, metal carbides, or carbon based, such as diamond-like carbon, graphite, graphite platelets, carbon-resin composites, conductive tin oxides. Coatings have to be compatible with the substrate bare metal and have good adhesion and peel resistance.

An additional requirement that has to be satisfied is a high level of surface hydrophilicity. Nonwettable plate surfaces result in unstable reactant flows that have to be countered with higher pressure drops and gas stoichiometries and hence higher parasitic power drains. This requirement has led to the development of hybrid coatings that can provide the low ICR and high wettability. At this time, the bipolar plates account for 75% of the total stack weight and x% of the stack cost. Table 4 summarizes some of the targets for bipolar plates for automotive fuel cells.

Future Directions

Direct hydrogen-fuel-cell-powered vehicles have reached a level of development where the major automotive companies have publicly announced that initial initiation of commercialization has begun. The targets of performance, durability, and cost agreed upon by various organizations, including the US DOE, appear to be achievable with recent improvements in stack and cell designs as shown in Figures 22, 23, and 24. Well-delineated pathways and strategies have been established to address the barriers of cost and durability of PEMFC stacks and achieve the automotive targets. The principal directions for reduction of cost and enhancement of durability of key fuel cell components, i.e., electrocatalysts, membranes, and bipolar plates are briefly summarized in this section.

Pt-based electrocatalysts will continue to be used in both the anode and cathode of automotive PEMFCs for the next decade. The current status of catalysts in automotive PEMFCs is a Pt-based carbon black-supported catalyst (20–50 wt.% Pt/C, 2–4 nm, 60–90 m^2/g) with a loading of 0.20–0.35 mg$_{\mathrm{Pt}}$/cm^2 on the cathode and about 0.05 mg/cm^2 on the anode. About 30 g of Pt are required for a 100-kW-rated stack. The rated power usually corresponds to a voltage of 0.60 V at 1–2 A/cm^2. The durability of fuel cell stacks under automotive conditions fall in the range of 3,500 h or 75% of the target life.

Progress has already been made over the years in enhancing the activity of the Pt nanoparticles dispersed on carbon support catalysts by alloying Pt with base metals such as Co, Ni, Fe, Rh, Cu, and Ti. The activity enhancements are a factor of 2–4, although the performance decreases over time. The Pt-alloys/C also fortuitously exhibit improved durability in part due to their larger particle size and heat treatment. This is a conventional pathway that has already been explored and proven over the last few decades in PTFE-bonded electrodes used in PAFCs. A correlation to the improved activity from alloying is that the oxygen binding weakens as the d-band center shifts [59–61]; a volcano plot of various metals can be obtained with Pt sitting at the top [62]. Also, an increased number of neighboring metal atoms, 3d metal neighbors, as well as compressive strain have all been reported to weaken the oxygen binding to Pt. A positive shift in the onset of oxide observed in cyclic voltammograms indicating oxophobic nature of the surface has also been

Polymer Electrolyte Membrane (PEM) Fuel Cells: Automotive Applications, Table 4 Technical targets for automotive PEMFC bipolar plates [48]

Characteristic	Units	2015 Status	2020 Targets
Cost[a]	$\$/kW_{net}$	7[b]	3
Plate weight	kg/kW_{net}	<0.4[c]	0.4
Plate H_2 permeation coefficient[d]	Std $cm^3/(sec\ cm^2 Pa)$ @ 80 °C, 3 atm 100% RH	0[e]	$<1\ 3 \times 10^{-14}$[f]
Corrosion, anode[g]	$\mu A/cm^2$	No active peak[h]	<1 and no active peak
Corrosion, cathode[i]	$\mu A/cm^2$	<0.1[c]	<1
Electrical conductivity	S/cm	>100[j]	>100
Areal specific resistance[k]	ohm cm^2	0.006[h]	<0.01
Flexural strength[l]	MPa	>34 (carbon plate)[m]	>25
Forming elongation[n]	%	20–40[o]	40

[a] Costs projected to high volume production (500,000 80 kW systems per year), assuming MEA meets performance target of 1,000 mW/cm^2

[b] Cost when producing sufficient plates for 500,000 systems per year. DOE Hydrogen and Fuel Cells Program Record 15,015, "Fuel Cell System Cost – 2015." http:www.hydrogen.energy.gov/program_records.html

[c] C.H. Wang (Treadstone), "Low-cost PEM Fuel Cell Metal Bipolar Plates." 2012 Annual Progress Report, http:www.hydrogen.energy.gov/pdfs/progress12/v_h_1_wang_2012.pdf

[d] Per the standard gas transport test (ASTM D1434)

[e] C.H. Wang (Treadstone), private communication, October 2014

[f] Blunk, et al. J. Power Sources 159 (2006) 533–542

[g] pH 3 0.1 ppm HF, 80 °C, peak active current $<1 \times 10^{-6}$ A/cm^2 (potentiodynamic test at 0.1 mV/s, −0.4 V to +0.6 V (Ag/AgCl)), de-aerated with Ar purge

[h] Kumar, M. Ricketts, and S. Hirano, "Ex-situ evaluation of nanometer range gold coating on stainless steel substrate for automotive polymer electrolyte membrane fuel cell bipolar plate," Journal of Power Sources 195 (2010): 1401–1407, September 2009

[i] pH 3 0.1 ppm HF, 80 °C, passive current $<5\times10^{-8} A/cm^2$(potentiodynamic test at +0.6 V (Ag/AgCl) for >24 h, aerated solution)

[j] O. Adrianowycz (GrafTech). "Next Generation Bipolar Plates for Automotive PEM Fuel Cells," 2009 Annual Progress Report. http:www.hydrogen.energy.gov/pdfs/progress09/v_2_adrianowycz.pdf

[k] Includes interfacial contact resistance (on as received and after potentiostatic test) measured both sides per Wang, et al. J. Power Sources 115 (2003) 243–251 at 200 psi (138 N/cm^2)

[l] ASTM-D 790–10 Standard Test Method for Flexural Properties of Unreinforced and Reinforced Plastics and Electrical Insulating Materials

[m] D. Haack et al. (Porvair), "Carbon-Carbon Bipolar Plates." 2007 Annual Progress Report, http:www.hydrogen.energy.gov/pdfs/progress07/v_b_3_haack.pdf

[n] Per ASTM E8M-01 Standard Test Methods for Tension Testing of Metallic Materials, or demonstrate ability to stamp generic channel design with width depth, and radius

[o] M. Brady et al. (Oak Ridge National Laboratory), "Nitrided Metallic Bipolar Plates." 2010 Annual Progress Report, http://www.hydrogen.energy.gov/pdfs/progress10/v_1_1_brady.pdf

directly correlated to enhanced ORR activity. Larger Pt particles, heat-treated Pt particles, and alloys of Pt exhibit oxophobic tendencies and concomitant improved activities. More recently, the understanding of the impact of d-band center on the metal-oxygen bond strength has been refined [63]; the entire valence band structure (density of states vs. binding energy) affects the bond strength and simplification of the band to a single "d-band center" is not valid. To summarize, the same binary and ternary alloys used previously in acid fuel cells are being implemented in PEMFCs using modified electrode structures.

A well-known weakness of the Pt-alloy approach is the leaching out of the base metal from the surface immediately and from the bulk over time. It has been shown by Stamenkovic et al. [64] that almost all the surface base metal is leached off once in contact with electrolyte; a Pt skeleton structure is formed (or Pt-skin for

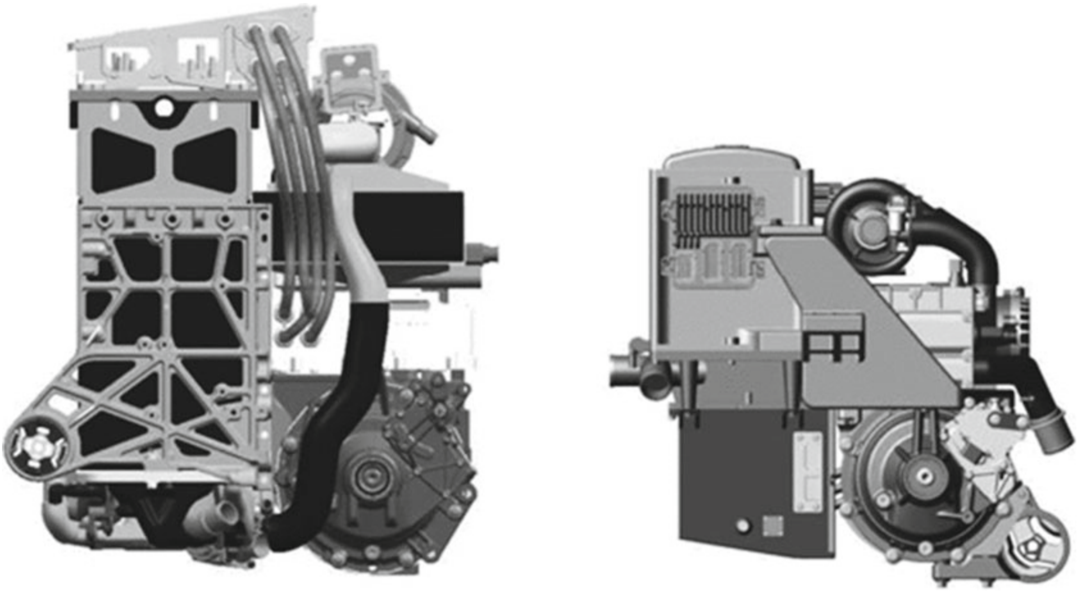

GENI FCS (GMT101X)		GEN2 FCS (GMT/E)
104	Stack Size (L)	64
80	Platinum (g)	30
405	System Size (L)	191
250	System Mass (kg)	130
62	Peak Power @ 150,000 miles (kW)	78
187	System Part Numbers	120
1903	System Part Count	1100

Polymer Electrolyte Membrane (PEM) Fuel Cells: Automotive Applications, Fig. 22 Demonstration of improvement in the automotive polymer electrolyte fuel cell stack and system

annealed catalysts) that has higher coordinated Pt atoms and a sublayer enriched in the base metal contributes to the higher activity. Nevertheless, as long as the catalyst activity and fuel cell performance is maintained within the target limits over the life of the stack, it remains an acceptable approach. Fundamental studies on single crystal Pt and Pt-alloys through a “materials by design” approach that involves the simultaneous application of a number of surface spectroscopies to a surface undergoing electrochemistry are being pursued by Markovic et al. [65]. Alloys with controlled crystal orientation such as the PtNi (111) have been demonstrated by Stamenkovic et al. [66] to show extremely high specific activities; it remains a fundamentally important yet difficult approach to implement in practical catalysts. Perturbations in the approach to the use of alloy catalysts are the use of voltammetrically dealloyed catalysts such as dealloyed $Pt_{25}Cu_{75}$ and $Pt_{20}Cu_{20}Co_{60}$ nanoparticles [67]. Pt-rich surfaces and alloy-rich cores of such materials have been shown to exhibit significantly improved activity for oxygen reduction in acidic media due to a reduced Pt-Pt atomic distance (lattice strain) and also possess superior durability to commercial Pt/C.

Two other pathways being explored to further drastically reduce the Pt loading are: (1) raising the catalyst mass activity (mA/mg) by using a core of base metal coated with monolayers of Pt and (2) applying the concept of high specific activity-extended thin films to a practical catalyst electrode system. The catalysts in the first pathway are often referred to as core-shell catalysts [68, 69].

Polymer Electrolyte Membrane (PEM) Fuel Cells: Automotive Applications, Fig. 23 Improvement in automotive fuel-cell system

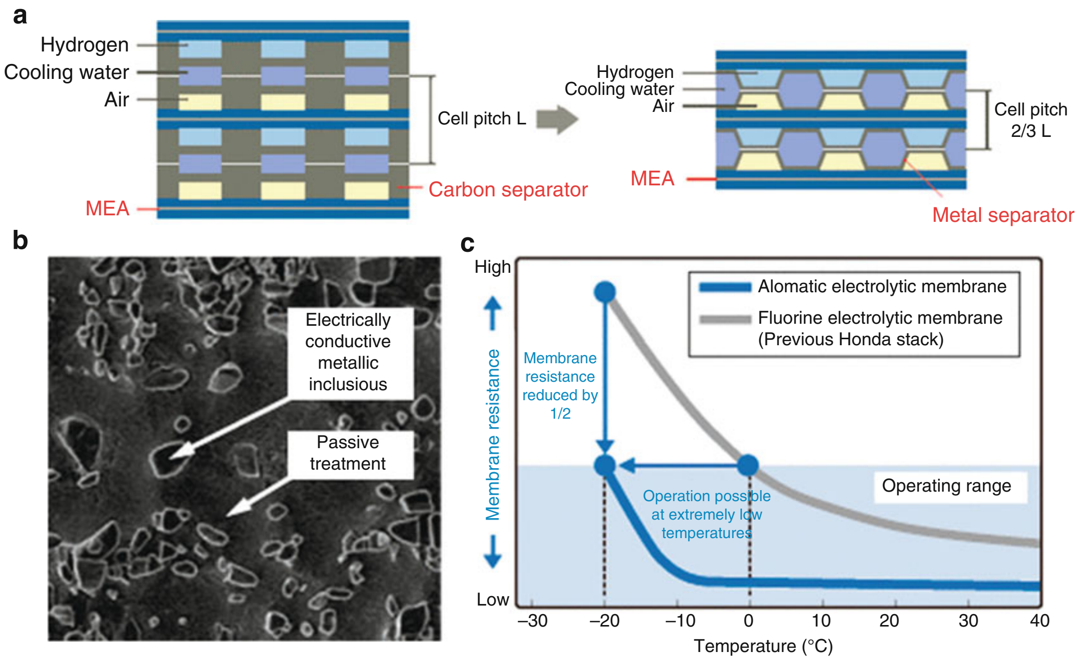

Polymer Electrolyte Membrane (PEM) Fuel Cells: Automotive Applications, Fig. 24 Improvement in automotive fuel-cell stack and system from Honda showing the advancements in cell bipolar plates and membranes

A deposition technique that involves the replacement of a first UPD metal adlayer with a 2D deposit of a nobler metal monolayer to cover the surface uniformly forms the basis of the technique [70]. In addition to the use of expensive Pt only at the surface where reaction takes place, the use of different subsurface materials enhance the specific activity of the surface Pt layer; a Pt-metal mixed surface monolayer may also be used. About 4–10× enhancement in mass activity has been shown using these catalysts. The use of small quantities of gold clusters [71] on the surface has also shown to enhance the durability of the catalysts under potential cycling. Latest work in the area includes the generation of hollow Pt spheres (4–8 nm hollow spheres having 1–2 nm Pt shells) prepared from Ni templates exhibiting 5× enhancement of activity over solid nanoparticles (measured in rotating disk electrode liquid electrolyte half cells) [72]. Scale-up and evaluation in fuel cells of several of these technologies is currently underway.

For decades, discussion on the enhanced specific activity of larger nanoparticles has raged. Larger nanoparticles of Pt have been found to have both a higher activity as well as a higher durability by several groups [38, 73, 74]. In addition, bulk polycrystalline Pt has been shown to have ~10× higher specific activity that Pt nanoparticle in half-cells using ultra pure nonadsorbing liquid electrolytes such as perchloric acid. Over the last decade, the high specific activity of continuous thin films has finally been demonstrated in practical MEAs of fuel cells especially by 3 M with their NSTF catalysts [75, 76]. Two challenges remain in the widespread use of these catalysts in practical fuel cells: the mass specific surface area (m^2/g) which is ten times lower for these films at this time and significant mass transport resistances due to flooding under humidified conditions due to the thinness of the cathode catalyst layer. Essentially, the catalyst films (~30 nm thick) are not thin enough to provide high mass activity and the electrode structure formed with these catalysts is not thick enough to disperse water easily. Both issues are being addressed by programs funded by the US DOE, and in laboratories elsewhere; the next 5 years will determine the degree of success of this approach [77]. - Figure 25 outlines the main precious metal pathways for future fuel cell electrocatalysts. One of the unexpected problems associated with the use of lower Pt loadings (with Pt-alloys/C) on the cathode is that a higher drop in high current density near peak power is observed compared to higher loaded catalysts. Although not fully resolved, it has been partially attributed to a local resistance at the catalyst ionomer interface as is being currently addressed by major automotive companies and research institutions.

Fundamental research related the formation of surface oxides on Pt [78–80] as well as Pt dissolution [81], although studied in the past, has come to the forefront again. This is due to the current understanding that the dissolution/surface area loss of Pt/C in automotive fuel cells is intensified by the cycling of load and hence potential [35, 40, 82] along with the trend toward core-shell and nanofilms of catalysts. Operational methods to limit the losses through this understanding of mechanisms as well as material solutions are being actively pursued [32].

An intermediate approach to limit the use of Pt and instead use Pd-based metal alloys has shown reasonable success in activity improvement. Although fairly precious, Pd is currently four times less expensive than Pt. Pd alloyed with Mo, Ta, W, Re, and Cu have all been evaluated. A Pd-Cu (1:1) catalyst composed of 20 nm nanoparticles prepared by co-impregnation showed activity within range of Pt and is being further pursued [63, 83].

Nonprecious metal catalysts (non-Pt group metals/non-PGM) research is still in its infancy and lags in activity and durability by a factor of ~10 compared to conventional Pt/C electrocatalysts; they have shown significant progress in terms of improved activity in recently reported work, and research in this field continues as a long-term approach to completely eliminate platinum usage in fuel cells. The target for non-PGM catalyst activity is expressed per unit volume (>130 A/cm^3 @800 mV) since it is the volume/electrode thickness that determines its usability. An example is the C|Fe|N catalyst system that can be synthesized by heat treatment of $Fe\text{-}N_4$ macrocycles as well as individual precursors of the three elements [84, 85]. Lefevre et al. [86] synthesized the catalyst system by utilizing ball-milling to fill microporous carbon with iron ions and pore fillers to obtain higher ORR activity. Carbon supported as well as sputtered transition metal (Cr, Co, Fe)/chalcogens (Se, S) have also been studied with limited success [87]. In research funded by the USDOE, heat-treated, carbon-supported polypyrrole and PANI in the presence of salts of Fe and Co are being investigated in half-cell rotating disk electrodes as well as subscale fuel cells. In comparison to carbon, pyrolyzed carbon, PANI/C, PANI-Co/C, PANI-Fe/C, PANI-Fe_3Co/C exhibited the highest ORR activity of 27 A/cm^3 at 800 mV under $H_2|O_2$; the peroxide yield for PANI-Fe_3Co/C was found to be the lowest at 0.5% [88]. A cyanamide-Fe-C (3.5 mg/cm^2) catalyst has shown catalyst activity in fuel cells of 165 A/cm^3 @ 800 mV in most recent work [89]. Much work remains to be carried out in the fundamental understanding and characterization of non-PGM catalysts

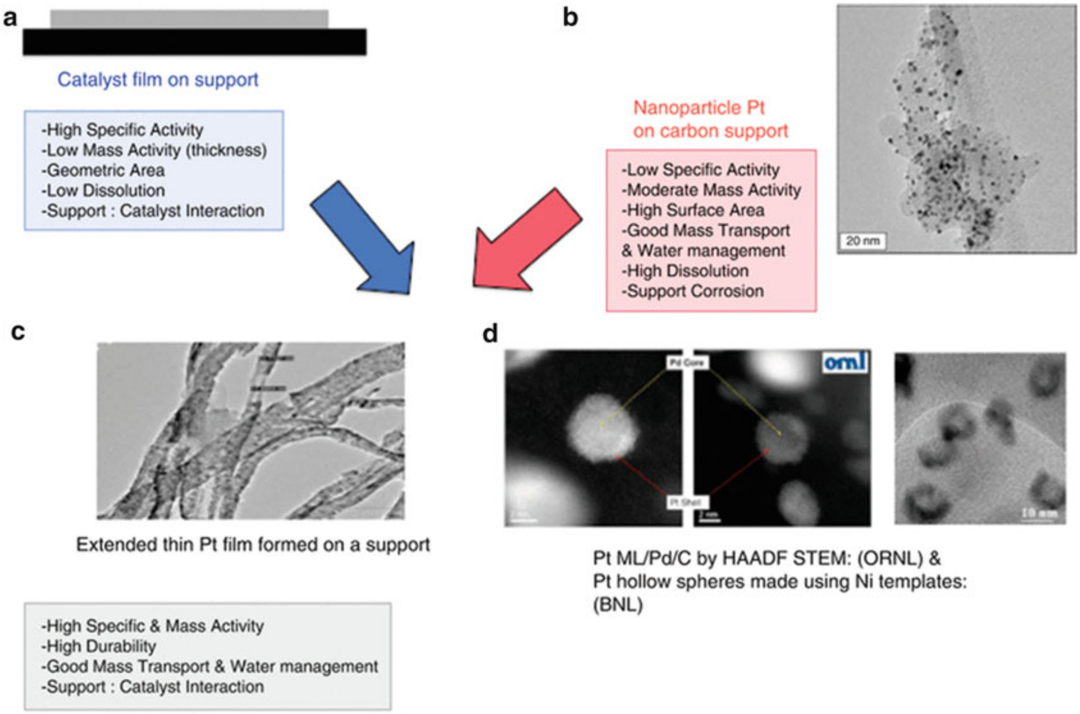

Polymer Electrolyte Membrane (PEM) Fuel Cells: Automotive Applications, Fig. 25 Pathways for future electrocatalyst development for automotive PEMFCs. (**a**) Thick films or bulk single crystal and polycrystalline catalysts that are ideal for fundamental studies on surface structure and mechanisms; these materials need to be modified into (**c**) and (**d**) to be applicable to fuel cells. (**b**) Typical commercial nanoparticles (2–4 nm) on a high-surface-area carbon support used in fuel cells at this time; (**c**) Thin continuous films of catalyst on a support such as carbon nanotubes that may provide a physical porous structure for mass transport in a fuel cell; (**d**) Core-shell catalysts where only the shell consists of precious metals and are supported on a typical high-surface-area support [72, 77, 89]

in terms of identification and quantification of the reaction sites and estimating the turnover frequencies and mechanisms for the ORR.

The high-surface-area carbon supports used today enable the use of small nanoparticles of Pt that are well-dispersed; the price paid in using a high-surface-area carbon black is that it tends to be susceptible to corrosion [90–93]. Carbon is thermodynamically susceptible to corrosion in the entire fuel cell operating regime but the kinetics are fortunately very slow. Near and above the open circuit potential of 0.95 V and especially above 1.1 V, the corrosion currents increase. Potentials in the range 1–1.5 V are seen only during uncontrolled start-up and shutdown of fuel cells [43, 94, 95]. Using mitigation techniques based on operating conditions, the highest potential seen is close to the OCV and the losses correspondingly lower. Nevertheless, some carbon corrosion is observed over the life of the fuel cell and material solutions are being actively sought. The material solutions will enable system simplification and lower costs. Alternative non-carbon supports such as titanium, tungsten oxides, nitrides, and borides are being studied that can provide a higher corrosion resistance at high potentials and also help anchor the Pt nanoparticles and limit degradation due to particle agglomeration. The main issues with alternative materials is that the corrosion resistance often comes with the cost of lower conductivity, lower surface area, different electrode structure, and the need for new methods to deposit catalysts on them.

Intensive research is being carried out to improve both the membrane performance (conductivity/areal resistance) and durability. The protonic conductivity is typically improved by the use of low EW ionomers; these ionomers swell with water to a greater extent increasing fatigue stresses. Thinner membranes are also being developed to reduce the areal resistance, but often need to be reinforced to provide mechanical strength and suffer from higher reactant permeability and susceptibility to shorting. Thus, a trade-off between performance and durability is often unavoidable.

Development of new membrane materials that have the capability of sustaining proton conduction under low RH conditions and at temperatures as high as 120 °C has been a struggle. Such a membrane would allow facile water management and also reduce thermal management issues in the stack. Of the two desired properties, a membrane that operates at low RH with sufficient conductivity is more critical since catalyst (both platinum and carbon) degradation is also suppressed under these conditions.

The approach to synthesizing new membrane material candidates involves obtaining the required properties of conductivity, chemical and mechanical durability by: tailoring or modifying water retention, domain interconnectivity, lowering the equivalent weight, use of additives such as metal composites and quenchers, stabilizing bonds and end group terminations, use of short side-chains, using reinforcements and cross-linking, raising the glass transition temperature, the use of amphoteric protogenic groups such as imidazole and phosphonic acid, etc. [96, 97]. Inorganics such as titania, silica, and zirconium phosphate have been incorporated into membranes in attempts to maintain conductivity at low RH through tightly bound water in these compounds. The use of amphoteric protogenic groups such as imidazole [98] and phosphonic acid that allow for proton transport in the absence of water has also been pursued [99]. PBI-PA-based membranes at temperatures above 200 °C have been investigated by several groups [100] and commercialized by PEMEAS®. These materials suffer from the leaching of phosphoric acid, complex start-up and shutdown, as well as loss of Pt activity due to phosphate anion adsorption. Modifications to this approach include the use of sulfonimides, perfluorinated acids, and metal oxides as additives to reduce the anion adsorption and increase the oxygen solubility. Heteropoly acids such as phosphotungstic acid, silicotungstic acid, and sulfonated zeolites have been used with partial success [101]. 10–20 wt.% heteropoly acids (not immobilized) were combined with 3 M PFSA ionomers to cast membranes and prepare MEAs; they showed a reduction in the FRR in fuel cell tests under hot dry conditions [100]. Additives in general may not be stable and may leach out over long periods of time and may also change the mechanical properties of the membrane. High-temperature, water-free/water-insoluble, proton-conducting membranes (protic salt polymer membranes) where a salt repeat unit conducts protons with an adjacent unit without the transport of water are also being researched by Gervasio et al. [102]. The membranes are prepared from solvent-free liquid salts known as protic ionic liquids or pILs that are tailored by selecting an acid and base.

Recently, the use of highly electron-poor poly (phenylene) backbones has resulted in ionomers containing sulfone ($-SO_2-$) units connecting the sulfonic acid ($-SO_3H$) functionalized phenyl rings that exhibit high proton conductivity and stability [103]. Some preparation routes have resulted in highly sulfonated material with an exchange capacity of IEC = 4.5 meq/g or an EW of 220 g/eq along with low water transport coefficients. These materials though are water soluble and brittle in the dry state but may still be usable as a component in a PEM. The task of synthesizing and developing such membranes is a difficult task, but even partial success such as obtaining a membrane that can operate at similar temperatures as today but at lower RH will help advance PEMFC stack technology considerably. Hydrophobic-hydrophilic multiblock copolymers ($BPSH_x$–BPS_y; where x = MW of sulfonated poly (arylene ether) and y = MW of poly(arylene ether)) with varying block lengths and controlled morphology that develop order and produce a co-continuous hydrophilic phase for good conductivity at low humidity have also been the subject of research as potential candidates for a new PEM [58].

Incremental engineering modification of membranes is also being carried out with some success. Composite membranes that consist of conductive and nonconductive porous polymer reinforcements have been incorporated for some time into membranes to provide mechanical strength for extremely low thicknesses; they suffer from some loss of conductivity. One approach is to form a composite/polymer blend and decouple the proton conduction from other membrane requirements. Arkema has demonstrated an inexpensive hydrocarbon-based polyelectrolyte blended with polyvinylidene difluoride (PVDF or Kynar) that exhibits similar performance to commercial PFSA membranes [104]. Another approach involves the use of electrospun ionomer fibers embedded in a polymer [105]. 3 M has reported the fabrication of 825 EW nonreinforced membranes with new additives that meet the targets of 20,000 RH cycles and 500 h OCV test in fuel cells [106]. Giner Electrochemical Systems [107] has reported on the development of dimensionally stable membranes (DSM) with laser-drilled supports composed of polysulfone or polyimide (Kapton) or that lowers the swelling of high acid content PFSA ionomers. Asahi Glass Co., [108, 109] has reported a new polymer composite membrane (based on PFSAs) in PEMFCs operating at 120 °C, 50% RH for ~4,000 h; the MEA tested in fuel cells had a degradation rate of 75 μV/h and a FRR of less than 1% of the baseline control. Chemical modification of PFSA membranes is being carried out to minimize the nonfluorinated end groups susceptible to degradation. Additives such as Ce^{3+} and Mn^{2+} ions added in trace quantities into the membrane and ionomer have also been demonstrated to improve the chemical stability.

Although the focus of this entry is on PEMs that are being used in automotive fuel cells today, brief mention must be made of work carried out on alkaline anion exchange membranes (AAEMs). Such membranes have the potential to exhibit sufficient activity when used with nonprecious metal catalysts, may work with fuels such as methanol and ethylene glycol, and provide some of the features that commercial PFSA membranes provide for PEMFCs. A cross-linked, water-insoluble, OH^--conducting, alkaline polymer free of metal ions and consisting of counter ions bound to the quaternary-ammonium containing polymer backbone has been reported with reasonable preliminary results (133–153 μm thick, 0.0092 S/cm @ 30 °C, 100%RH) [110]. H_2|Air alkaline membrane fuel cells that showed encouraging preliminary results with Pt and transition metal catalyst cathodes in CO_2 free air have also been reported recently by Acta S.p.A [111].

Graphite-based bipolar plates have been used in PEMFC stacks, they suffer from drawbacks such as higher manufacturing costs, greater thicknesses, higher gas permeability that is necessary for high power density automotive fuel cell stacks. Metal bipolar plates (stainless steel, Ni, Ti, Al-based alloys) on the other hand possess high thermal conductivity, high mechanical and flexural strength, and facile high volume production but tend to corrode and require corrosion-resistant and conductive coatings that increase their cost [112]. New coatings are under development along with thinner stamped plates with most of the details being proprietary at this time. An example is thermal nitriding of thin (0.1 mm foils, Fe-20Cr-4 V and type 2205) stainless steel plates to generate surface layers of Cr_2N, CrN, TiN, V_2N, etc., that lowers the interfacial contact resistance and raises the corrosion resistance simultaneously [113]. The additional requirement of hydrophilicity to facilitate water management in the flow fields has led to the development of hybrid coatings that is capable of providing a low ICR and high wettability. Superhydrophilicity has been shown by layer-by-layer deposition of silica nanoparticles onto bipolar plates, which meets the other requirements [114]. Electrostatic layer-by-layer techniques have been employed to generate 100 nm coating structures that are constituted from 5 to 10 nm graphite platelets and 19 nm silica nanospheres. A low ICR of 4 mΩ-cm^2 and a high degree of hydrophilicity are simultaneously achieved by this method.

Figure 23 in the previous section showed the improvement in Nissans latest generation stack achieved by using metal separators instead of carbon. Figure 24 illustrates schematically novel surface treatments on stainless steel bipolar plates along with electrically conductive inclusions that help maintain high conductivity and corrosion resistance at the same time. Intensive applied research is being carried out to obtain thin, corrosion-resistant conductive bipolar plates modified with coatings that are inexpensive and conducive to high-speed/high-volume manufacturing.

A combination of synergistic improvements in the catalyst, support, gas diffusion layers, membrane, and essentially the entire porous electrode structure in conjunction with bipolar plates/flow fields is expected to improve the mass-transport of reactant gases, protons, and water management. Thus, an increase in the peak current density (A/cm^2) and peak power density (W/cm^2) will result; this in turn will lower the stack volume, the amount of catalyst, and membrane material used and raise the kW/L, kW/kg, and lower the $/kW stack metrics. It should be noted that the rated or peak power for automotive stacks is based in part on maintaining an electrical efficiency of $>50\%$; this dictates that the cell voltage has to be maintained above ~ 0.60 V. At this time, volumetric power densities of practical stacks in fuel cell vehicles have been reported to be as high as ~ 2 kW/L [46] and are likely to increase over the next few years contributing to lower stack costs ($/kW).

Trends in short- and longer-term directions for key fuel cell components including electrocatalysts/supports, membranes, and bipolar plates have been elaborated in this section; improvement of the performance and durability of these components will directly impact the entire automotive fuel cell system requirements, complexity, and cost. Durable catalysts with enhanced ORR activity, durable membranes that perform at very low humidity, and durable bipolar plates that have low contact resistance will not only increase the power density and cost of the fuel cell stack but also simplify and lower/eliminate system component costs of the air compressor, humidification systems, recycle pumps, radiator, start-up/shutdown and freeze-start-related components, etc. A combination of advances in all the fuel cell components discussed above, system simplification, governmental policies that are sensitive to sustainable clean energy, and development of a hydrogen infrastructure will enable achieving the projected technical and cost targets needed for automotive fuel cell commercialization.

Bibliography

Primary Literature

1. Grove WR (1842) On gaseous voltaic battery. Philos Mag 3:417
2. Schonbein CF (1839) On the voltaic polarization of certain solid and fluid substances. Philos Mag 14:43
3. Mond L, Langer C (1889) A New Form of Gas Battery. Proc Roy Soc 46:296
4. Jacques WW (1897) Electricity direct from coal. Harpers Mag 94:144–150
5. Baur E, Tobler J (1933) Brennstoffketten Z Elektrochem 39:169–180
6. Schmidt TJ, Paulus UA, Gasteiger HA, Behm RJ (2001) Peroixde rde, anion adsorption effect. J Electroanal Chem 508:41–47
7. Tobler J (1933) Studien Über Knallgas-Ketten. Z Elektrochem 39:148
8. Nernst W (1904) Theorie der Reaktiongeschwindigkeit in heterogenen Systemen. Z Phys Chem 47:52
9. Tafel J, Emmert B (1905) Ueber die ursache der spontanen depression des kathodenpotntials bei der eletrolyse verduennter schwefelsaeure. Z Phys Chem 50:349–373
10. Liebhavsky HA, Cairns EJ (1968) Fuel cells and batteries. Wiley, New York
11. Vielstich W (1965) Fuel cells. Wiley-Interscience, London
12. Maget HJR (1967) In: Berger C (ed) Handbook of fuel cell technology. Prentice-Hall, Englewood Cliffs, pp 425–491
13. Liebhavsky HA, Grubb WT Jr (1961) The fuel cell in space. ARS J 31:1183–1190
14. AFC A (2003) Alkaline fuel cells. In: Vielstich W, Lamm A, Gasteiger H (eds) Handbook of fuel cells-fundamentals, technology and applications. Wiley, New York
15. Kordesch KV (1978) 25 years of fuel cell development (1951–1976). J Electrochem Soc 125:77 C–91 C
16. Grubb WTJ (1959) US Patent 2,913,511
17. Niedrach LW, Alford HR (1965) A new high-performance fuel cell employing conducting-porous-teflon electrodes and liquid electrolyte. J Elecrochem Soc 112:117
18. Thomas CES (2007) Greenhouse gas results. http://www.cleancaroptions.com/html/greenhouse_gas_results.html
19. DOE US (2010) Well-to-wheels greenhouse gas emissions. http://www.hydrogen.energy.gov/pdfs/9002_well-to-wheels_greenhouse_gas_emissions_petroleum_use.pdf
20. IPCC (2007) The IPCC assessment reports. http://www.ipcc.ch/

21. Koppel T (1999) Powering the future: the ballard fuel cell and the race to change the world. Wiley, New York
22. Taub A (2009) The opportunity in electric transportation. http://www.ncsc.ncsu.edu/cleantransportation/docs/Events/2009_5-27_Taub_GM-EV.pdf
23. GreenCarCongress: GM highlights engineering advances with second generation fuel cell system and fifth generation stack; poised for production around 2015. http://www.greencarcongress.com/2009/09/gm-2gen-20090928.html
24. ChevyEquinox (2010) Chevy equinox fuel cell. http://www.gm.com/vehicles/innovation/fuel-cells/
25. AutoBlogGreen (2010) 2008 chevy equinox fuel cell. http://green.autoblog.com/photos/2008-chevrolet-equinox-fuel-cell/#380179
26. UTCPower (2010) UTC power: transportation\automotive. http://www.utcpower.com/fs/com/bin/fs_com_Page/0,11491,0151,00.html
27. F-cell M-BB-c (2010) 2010 mercedes-benz b-class f-cell. http://www.caranddriver.com/news/car/09q3/2010_mercedes-benz_b-class_f-cell-car_news
28. FCHV-adv T (2010) Fuel cell technology. http://www2.toyota.co.jp/en/tech/environment/fchv/
29. Pressroom T (2010) Toyota fuel cell vehicle demonstration program expands. http://pressroom.toyota.com/pr/tms/toyota/toyota-fuel-cell-vehicle-demonstration-151146.aspx
30. NissanHistory (2010) The history of Nissan's fuel-cell vehicle development. http://www.nissan-global.com/EN/ENVIRONMENT/CAR/FUEL_BATTERY/DEVELOPMENT/FCV/index.html
31. Honda (2010) Honda: fuel cell electric vehicle. http://world.honda.com/FuelCell/
32. Uchimura M, Sugawara S, Suzuki Y, Zhang J, Kocha SS (2008) Electrocatalyst durability under simulated automotive drive cycles. ECS Trans 16:225–234
33. Kocha SS (2003) Principles of mea preparation. In: Vielstich W, Lamm A, Gasteiger H (eds) Handbook of fuel cells-fundamentals, technology and applications. Wiley, New York, pp 538–565
34. Kocha SS, Yang DJ, Yi JS (2006) Characterization of gas crossover and its implications in PEM fuel cells. AIChE J 52:1916–1925
35. Uchimura M, Kocha S (2007) The impact of cycle profile on PEMFC durability. ECS Trans 11:1215–1226
36. Ohma A, Suga S, Yamamoto S, Shinohara K (2007) Membrane degradation behavior during OCV hold test. J Electrochem Soc 154:B757–B760
37. Sugawara S, Maruyama T, Nagahara Y, Kocha SS, Shinohara K, Tsujita K, Mitsushima S, Ota K-i (2009) Performance decay of proton-exchange membrane fuel cells under open circuit conditions induced by membrane decomposition. J Power Sources 187:324–331
38. Gasteiger HA, Kocha SS, Sompalli B, Wagner FT (2005) Activity benchmarks and requirements for pt, pt-alloy, and non-pt oxygen reduction catalysts for PEMFCS. Appl Catal B Environ 56:9–35
39. Mathias MF, Makharia R, Gasteiger HA, Conley JJ, Fuller TJ, Gittleman CJ, Kocha SS, Miller DP, Mittelsteadt CK, Tao X, Yan SG, PT Y (2005) Two fuel cell cars in every garage? Electrochem Soc Interface 14:24–35
40. Uchimura M, Kocha SS (2007) The impact of oxides on activity and durability of PEMFCS. AIChE J. Abstract No. 295b
41. Uchimura M, Kocha SS (2008) The influence of Pt-oxide coverage on the ORR reaction order in PEMFCs. ECS meeting, Honolulu, 12–17 Oct 2008
42. Kocha SS, Gasteiger HA (2004) The use of Pt-alloy catalyst for cathodes of PEMFCS to enhance performance and achieve automotive cost targets. Fuel Cell Seminar, San Antonio
43. Reiser CA, Bregoli L, Patterson TW, Yi JS, Yang JD, Perry ML, Jarvi TD (2005) A reverse-current decay mechanism for fuel cells. Electrochem Solid-State Lett 8:A273–A276
44. Reiser CA, Yang D, Sawyer RD (2005) Procedure for shutting down a fuel cell system using air purge. US Patent 6,858,336, 22 Feb 2005
45. Reiser CA, Yang DJ, Sawyer RD (2005) Procedure for starting up a fuel cell system using a fuel purge. US Patent 7,410,712, 12 Aug 2008
46. Shimoi R, Aoyama T, Iiyama A (2009) Development of fuel cell stack durability based on actual vehicle test data: current status and future work. SAE International 2009-01-1014
47. Merzougui B, Halalay IC, Carpenter MK, Swathirajan S (2006) Conductive matrices for fuel cell electrodes. General motors, US Patent Application 20060251954
48. DOE US (2007) Fuel cell targets. http://www1.eere.energy.gov/hydrogenandfuelcells/mypp
49. Borup RL, Meyers JP, Pivovar B, Kim YS, Mukundan R, Garland N, Myers DJ, Wilson M, Garzon F, Wood DL, Zelenay P, More K, Stroh K, Zawodizinski TA, Boncella J, McGrath J, Inaba M, Miyatake K, Hori M, Ota K-i, Ogumi Z, Miyata S, Nishikata A, Siroma Z, Uchimoto Y, Yasuda K, Kimijima K-i, Iwashita N (2007) Scientific aspects of polymer electrolyte fuel cell durability and degradation. Chem Rev 107:3904–3951
50. Mohtadi R, Lee WK, Zee JWV (2004) So_2 contamination. J Power Sources 138:216–225
51. Nagahara Y, Sugwara S, Shinohara K (2008) The impact of air contaminants on PEMFC performance and durability. J Power Sources 182:422–488
52. Kocha SS, Gasteiger HA (2004) In: Henry B (ed) Platinum alloy catalysts for PEMFCs. Gonzalez Convention Center, San Antonio. http://www.fuelcellseminar.com/past-conferences/2004.aspx
53. Satyapal S (2009) Hydrogen program overview. http://www.hydrogen.energy.gov/pdfs/review09/program_overview_2009_amr.pdf
54. Satyapal S (2009) Fuel cell project kickoff. http://www1.eere.energy.gov/hydrogenandfuelcells/pdfs/satyapal_doe_kickoff.pdf

55. NEDO (2007) Nedo homepage. http://www.nedo.go.jp/nenryo/gijutsu/index.html:
56. Iiyama A, Shinohara K, Igushi S, Daimaru A (2009) Membrane and catalyst performance targets for automotive fuel cells. In: Vielstich W, Gasteiger HA, Yokokawa H (eds) Handbook of fuel cells-advances in electrocatalysis, materials, diagnostics and durability. Wiley, Chichester
57. Cleghorn S, Griffith M, Liu W, Pires J, Kolde J (2007) Gore's development path to a commercial automotive membrane electrode assembly. http://www.fuelcellseminar.com/past-conferences/2007.aspx
58. McGrath J (2007) Advanced materials for proton exchange membranes. DOE Hydrogen Program Merit Review Presentation. http://www.hydrogen.energy.gov/pdfs/review07/fc_23_mcgrath.pdf
59. Luczak FJ (1976) Determination of d-band occupancy in pure metals and supported catalysts by measurement of the liii x-ray absorption threshold. J Catal 43:376–379
60. Mukerjee S, Srinivasan S, Soriaga MP, McBreen J (1995) Role of structural and electronic properties of Pt and Pt alloys on electrocatalysis of oxygen reduction. J Electrochem Soc 142:1409–1422
61. Nagy Z, You H (2002) Applications of surface x-ray scattering to electrochemistry problems. Electrochim Acta 47:3037–3055
62. Jalan V, Taylor EJ (1983) Importance of interatomic spacing in catalytic reduction of oxygen in phosphoric acid. J Electrochem Soc 130:2299–2302
63. Myers D (2009) http://www.hydrogen.energy.gov/pdfs/review09/fc_20_myers.pdf
64. Stamenkovic VR, Fowler B, Mun BS, Wang G, Ross PN, Lucas CA, Markovic NM (2007) Improved oxygen reduction activity on Pt3Ni(111) via increased surface site availability. Science 315:494–497
65. Markovic NM, Ross PN (2000) Electrocatalysts by design: from the tailored surface to a commercial catalyst. Electrochim Acta 45:4101–4115
66. Stamenkovic VR, Mun BS, Arenz M, Mayrhofer KJJ, Lucas CA, Wang G, Ross PN, Markovic NM (2007) Trends in electrocatalysis on extended and nanoscale Pt-bimetallic alloy surfaces. Nat Mater 6:241–247
67. Neyerlin KC, Srivastava R, Yu C, Strasser P (2009) Electrochemical activity and stability of dealloyed Pt-cu and Pt-cu-co electrocatalysts for the oxygen reduction reaction. J Power Sources 186:261–267
68. Zhang J, Lima FHB, Shao MH, Sasaki K, Wang JX, Hanson J, Adzic RR (2005) Pt monolayer on noble metal-noble metal core core-shell nanoparticle electocatalysts for O_2 reduction. J Phys Chem B 109:22701–22704
69. Zhang J, Mo Y, Vukmirovic MB, Klie R, Sasaki K, Adzic RR (2004) Pt-Pd core-shell. J Phys Chem B 108:10955
70. Brankovic SR, Wang JX, Adzic RR (2001) Metal monolayer deposition by replacement of metal adlayers on electrode surfaces. Surf Sci 474: L173–L179
71. Zhang J, Sasaki R, Sutter E, Adzic RR (2007) Stabilization of platinum oxygen reduction electrocatalysts using gold clusters. Science 315:220–222
72. Adzic RR (2010) Contiguous platinum monolayer oxygen reduction electrocatalysts on high-stability-low-cost supports. http://www.hydrogen.energy.gov/pdfs/review10/fc009_adzic_2010_o_web.pdf
73. Bregoli LJ (1978) The influence of platinum crystallite size on the electrochemical reduction of oxygen in phosphoric acid. Electrochim Acta 23:489–492
74. Makharia R, Kocha SS, PT Y, Sweikart MA, Gu W, Wagner FT, Gasteiger HA (2006) Durable PEMFC electrode materials: requirements and benchmarking methodologies. ECS Trans 1:3–18
75. Debe M (2005) Advanced meas for enhanced operating conditions, amenable to high volume manufacture. DOE hydrogen program review. http://www.hydrogen.energy.gov/pdfs/review05/fc3_debe.pdf
76. Debe M (2008) Advanced cathode catalysts and supports for pem fuel cells. http://www.hydrogen.energy.gov/pdfs/review08/fc_1_debe.pdf
77. Pivovar B (2010) Extended, continuous pt nanostructures in thick, dispersed electrodes. http://www.hydrogen.energy.gov/pdfs/review10/fc007_pivovar_2010_o_web.pdf
78. Conway BE (1995) Electrochemical oxide film formation at noble metals as a surface-chemical process. Prog Surf Sci 49:331–452
79. Conway BE, Barnett B, Angerstein-Kozlowska H (1990) A surface-electrochemical basis for the direct logarithmic growth law for initial stages of extension of anodic oxide films formed at noble metals. J Chem Phys 93:8361–8373
80. Conway BE, Jerkiewicz G (1992) Surface orientation dependence of oxide film growth at platinum single crystals. J Electroanal Chem 339:123–146
81. Bindra P, Clouser SJ, Yeager E (1979) Pt dissolution in concentrated phosphoric acid. J Electrochem Soc 126:1631
82. Wang X, Kumar R, Myers DJ (2006) Effect of voltage on platinum dissolution relevance to polymer electrolyte fuel cells. Electrochem Solid-State Lett 9:A225–A227
83. Wang X, Kariuki N, Vaughey JT, Goodpastor J, Kumar R, Myers DJ (2008) Bi-metallic Pd-cu oxygen reduction electrocatalysts. J Electrochem Soc 155:B602–B609
84. Jaouen F, Charreteur F, Dodolet JP (2006) C-n4. J Electrochem Soc 153:A689
85. Medard C, Lefevre M, Dodolet JP, Jaouen F, Lindbergh G (2006) C-n4. Electrochim Acta 51:3202
86. Lefevre M, Proietti E, Jaouen F, Dodolet J-P (2009) Iron-based catalysts with improved oxygen reduction activity in polymer electrolyte fuel cells. Science 324:71
87. Campbell S (2005) Development of transition metal/chalcogen based cathode catalysts for PEM fuel cells.

http://www.hydrogen.energy.gov/pdfs/review05/fc13_campbell.pdf
88. Zelaney P (2009) Advanced cathode catalysts. http://www.hydrogen.energy.gov/pdfs/review09/fc_21_zelenay.pdf
89. Zelaney P (2010) Advanced cathode catalysts. http://www.hydrogen.energy.gov/pdfs/review10/fc005_zelenay_2010_o_web.pdf
90. Bett JA, Kinoshita K, Stonehart P (1974) Crystallite growth of Pt dispersed on graphitized carbon black. J Catal 35:307–316
91. Bett JA, Kinoshita K, Stonehart P (1976) Crystallite growth of Pt dispersed on graphitized carbon black ii effect of liquid environment. J Catal 41:124–133
92. Cai M, Ruthkosky MS, Merzougui B, Swathirajan S, Balogh MP, Oh SH (2006) Investigation of thermal and electrochemical degradation of fuel cell catalysts. J Power Sources 160:977–986
93. Kinoshita K (1988) Carbon electrochemical and physicochemical properties. Wiley, New York
94. Yu PT, Gu W, Makharia R, Wagner F, Gasteiger H (2006) The impact of carbon stability on PEM fuel cell start-up and shutdown voltage degradation. ECS 210th Meeting, Abstract 0598.pdf. http://www.electrochem.org/meetings/scheduler/abstracts/210/0598.pdf
95. Yu PT, Kocha SS, Paine L, Gu W, Wagner FT (2004) The effects of air purge on the degradation of PEMFCS during startup an shutdown procedures. Proceedings of AIChE 2004 Annual Meeting, New Orleans, 25–29 Apr 2004
96. Kreuer KD, Paddison SJ, Spohr E, Schuster M (2004) PEM review. Chem Rev 104:4637–4678
97. Kreuer KD, Schuster M, Obliers B, Diat O, Traub U, Fuchs A, Klock U, Paddison SJ, Maier J (2008) Short-side-chain proton conducting perfluorosulfonic acid ionomers: why they perform better in PEM fuel cells. J Power Sources 178:499–509
98. Schuster MFH, Meyer WH, Schuster M, Kreuer KD (2004) Toward a new type of anhydrous organic proton conductor based on immobilized imidazole. Chem Mater 16:329–337
99. Steininger H, Schuster M, Kreuer KD, Kaltbeitzel A, Bingol B, Meyer WH, Schauff S, Brunklaus G, Maier J, Spiess HW (2007) Intermediate temperature proton conductors for PEM fuel cells based on phosphonic acid as protogenic group: a progress report. Phys Chem Chem Phys 9:1764–1773
100. Larson JM, Hamrock SJ, Haugen GM, Pham P, Lamanna WM, Moss AB (2007) Membranes based on basic polymers and perfluorinated acids for hotter and drier fuel cell operating conditions. J Power Sources 172:108–114
101. Meng FQ, Aieta NV, Dec SF, Horan JL, Williamson D, Frey MH, Pham P, Turner JA, Yandrasits MA, Hamrock SJ, Herring AM (2007) Structural and transport effects of doping perfluorosulfonic acid polymers with the heteropoly acids, h3pw12o40 or h4siw12o40. Electrochim Acta 53:1372–1378
102. Gervasio D (2010) Protic salt polymer membranes. http://www.hydrogen.energy.gov/pdfs/review09/fc_06_gervasio.pdf
103. de Araujo CC, Kreuer KD, Schuster M, Portale G, Mendil-Jakani H, Gebel G, Maier J (2009) Poly (p-phenylene sulfone)s with high ion exchange capacity: ionomers with unique microstructural and transport features. Phys Chem Chem Phys 11:3305–3312
104. Yi J (2007) Development of low-cost, durable membrane and MEA for stationary and mobile fuel cell applications. http://www.hydrogen.energy.gov/pdfs/review07/fc_9_yi.pdf
105. Pintauro P (2010) Nanocapillary network proton conducting membranes for high temperature hydrogen/air fuel cells. http://www.hydrogen.energy.gov/pdfs/review10/fc038_pintauro_2010_o_web.pdf
106. Hamrock SJ (2010) Membranes and meas for dry, hot operating conditions. http://www.hydrogen.energy.gov/pdfs/review10/fc034_hamrock_2010_o_web.pdf
107. Mittelsteadt CK (2010) Dimensionally stable membranes. http://www.hydrogen.energy.gov/pdfs/review10/fc036_mittelsteadt_2010_o_web.pdf
108. Endoh E (2008) Progress of highly durable mea for PEMFC under high temperature and low humidity conditions. ECS Trans 12:41–50
109. Endoh E, Terazono S, Widjaja H, Takimoto Y (2004) OCV degradation. Electrochem Solid-State Lett 7: A209–AA211
110. Varcoe JR, Slade RCT, Yee E (2006) An alkaline polymer electrochemical interface: a breakthrough in application of alkaline anion-exchange membranes in fuel cells. Chem Commun 6:1428–1429
111. Piana M, Boccia M, Filipi A, Flammia E, Miller HA, Orsini M, Salusti F, Santiccioli S, Ciardelli F, Pucci A (2010) H_2/air alkaline membrane fuel cell performance and durability, using novel ionomer and non-Pt group metal cathode catalyst. J Power Sources 195:5875–5881
112. Wang H, Turner JA (2010) Reviewing metallic PEMFC bipolar plates. Fuel Cells 10:510–519
113. Brady MP, Wang H, Turner JA, Meyer HM, More KL, Tortorelli PF, McCarthy BD (2010) Pre-oxidized and nitrided stainless steel alloy foil for proton exchange membrane fuel cell bipolar plates: part 1. Corrosion, interfacial contact resistance, and surface structure. J Power Sources 195:5610–5618
114. Dadheech G, Elhamid MHA, Blunk R (2009) Nanostructured and self-assembled superhydrophilic bipolar plate coatings for fuel cell water management. Nanotech Conference & Expo 2009, vol 3, Technical Proceedings, Austin, TX, pp 18–183

Books and Reviews

Alsabet M, Grden M, Jerkiewicz G (2006) Comprehensive study of the growth of thin oxide layers on pt electrodes under well-defined temperature, potential, and time conditions. J Electroanal Chem 589:120–127

Bard AJ, Faulkner LR (1980) Electrochemical methods. Wiley, New York

Bockris JO'M, Reddy AKN (1973) Modern electrochemistry: an introduction to an interdisciplinary area, vol 1. Springer, New York

Borup RL, Meyers JP, Pivovar B, Kim YS, Mukundan R, Garland N, Myers DJ, Wilson M, Garzon F, Wood DL, Zelenay P, More K, Stroh K, Zawodizinski TA, Boncella J, McGrath J, Inaba M, Miyatake K, Hori M, Ota K-i, Ogumi Z, Miyata S, Nishikata A, Siroma Z, Uchimoto Y, Yasuda K, Kimijima K-i, Iwashita N (2007) Scientific aspects of polymer electrolyte fuel cell durability and degradation. Chem Rev 107:3904–3951

Conway BE (1952) Electrochemical data. Greenwood Press, Westport

Conway BE (1964) Theory of principles of electrode processes. Ronald Press, New York

Conway BE (1995) Electrochemical oxide film formation at noble metals as a surface-chemical process. Prog Surf Sci 49:331–452

Conway BE, Jerkiewicz G (1992) Surface orientation dependence of oxide film growth at platinum single crystals. J Electroanal Chem 339:123–146

Gileadi E (1993) Electrode kinetics. VCH, New York

Kinoshita K (1988) Carbon electrochemical and physicochemical properties. Wiley, New York

Kinoshita K (1992) Electrochemical oxygen technology. Wiley, New York

Kocha SS (2003) Principles of MEA preparation. In: Vielstich W, Lamm A, Gasteiger H (eds) Handbook of fuel cells-fundamentals, technology and applications. Wiley, New York, pp 538–565

Kocha SS, Yang DJ, Yi JS (2006) Characterization of gas crossover and its implications in PEM fuel cells. AICHE J 52:1916–1925

Koppel T (1999) Powering the future: the ballard fuel cell and the race to change the world. Wiley, New York

Kreuer KD, Paddison SJ, Spohr E, Schuster M (2004) Pem review. Chem Rev 104:4637–4678

Liebhavsky HA, Cairns EJ (1968) Fuel cells and batteries. Wiley, New York

Markovic NM, Ross PN (2000) Electrocatalysts by design: from the tailored surface to a commercial catalyst. Electrochim Acta 45:4101–4115

Mathias MF, Makharia R, Gasteiger HA, Conley JJ, Fuller TJ, Gittleman CJ, Kocha SS, Miller DP, Mittelsteadt CK, Tao X, Yan SG, Yu PT (2005) Two fuel cell cars in every garage? Electrochem Soc Interface 14:24–35

Mench MM (2008) Fuel cell engines. Wiley, Hoboken

Pourbaix M (1966) Atlas of electrochemical equilibrium in aqueous solutions, 1st edn. Pergamon Press, New York

Prentice G (1991) Electrochemical engineering principles. Prentice Hall, Englewood

Savadogo O (1998) Emerging membranes for the electrochemical systems: (i) solid polymer electrolyte membranes for fuel cell systems. J New Mater Electrochem Syst:47–66

Vetter KJ (1963) A general thermodynamic theory of the potential of passive electrodes and its influence on passive corrosion. J Electrochem Soc 110:597–605

Wilson MS, Gottesfeld S (1992) High performance catalyzed membranes of ultra-low Pt loadings for polymer electrolyte fuel cells. J Electrochem Soc 139:L28–L30

Zawodzinski TA, Derouin CR, Radzinski S, Sherman RJ, Smith VT, Springer TE, Gottesfeld S (1993) Water uptake by and transport through nafion 117 membranes. J Elecrochem Soc 140:1041–1047